

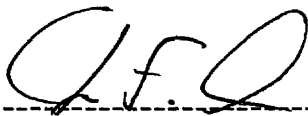
**Effects of Age and Retinal Degeneration on the Expression of
Subtilisin-Like Proprotein Convertases in the Visual Cortex of
Mice**

by

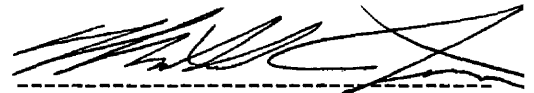
Krishnapriya Chinnaswamy

Thesis submitted to the Faculty of the
University of Michigan –Flint
in partial fulfillment of the
requirements for the degree of
Master of Science in Biology

Approved By:



Dr. Joseph F. Sucic
Thesis Adviser
Dept. of Biology



Dr. Michael Jarvinen
Thesis Adviser
Dept. of Psychology
Emmanuel College



Dr. Ann Sturtevant
Reader
Dept. of Biology

University of Michigan-Flint
June 2009

Effects of Age and Retinal Degeneration on the Expression of Subtilisin-Like Proprotein Convertases in the Visual Cortex of Mice

by

Krishnapriya Chinnaswamy

Joseph F. Sucic

Chairman Biology

Abstract

Postnatal development of the visual cortex is a complex process that involves a number of molecules like growth factors, neuropeptides and cholesterol. Neurotrophins, like NGF, BDNF, NT-3 and NT-4, which are synthesized as precursors, also play a very important role in visual cortex development. Subtilisin-like proprotein convertases (SPCs) play a vital role in the limited endoproteolysis of precursors of secretory proteins that participate in development, homeostasis and in numerous pathologies. SPCs also process pro-neurotrophins into mature forms which facilitates neuron survival and differentiation through binding of the neurotrophins Trk receptors. In contrast, unprocessed forms of neurotrophins bind to the p75NTR death receptor and cause apoptosis. We studied the expression pattern of SPCs during postnatal development of the visual cortex in wild type mice (wt) and retinal degeneration mice (rd) using quantitative real-time PCR. The widely expressed SPCs showed a similar pattern of expression during development with high levels of mRNA early in postnatal development

The expression pattern of SPCs was totally different in rd mice. Lower levels of expression of both widely expressed and tissue-specific SPCs were seen at week 1. PCSK9 also showed a significant difference in expression. PCSK9 might play an important role in synaptic formation by regulating the uptake of cholesterol. This difference in expression pattern of SPCs during development and retinal degeneration support the hypothesis that SPCs play a critical role during brain development and neurodegenerative diseases. Understanding the potential role of SPCs in neurodegenerative diseases may lead to new targets for treating such diseases.

Acknowledgements

First, I would like to thank my family for giving me this opportunity to study in United States, which was my dream. I also thank them for their support and constant encouragement. Next, I would like to thank my fiancé, Arasakumar Subramani, for his love and support. He was the only relation that I had in US and without him I would not have survived here. I also thank Dr. Joseph Sucic for allowing me to work in his lab and answering my questions patiently. He was like a friend rather than a professor and I really enjoyed working in his lab. Thank you Dr. Sucic. Next, I want to thank Dr. Michael Jarvinen for letting me work on his project and helping me in statistics and graphs. When I heard that he was going to Boston, I was bit worried about my thesis because he was the main part of this project. However, even though he was in Boston, he really helped me with everything by having phone conferences and visiting here whenever he got the chance. I thank Dr. Ann Sturtevant for agreeing to be in my thesis committee and also helping in cloning and sequencing the PCR products. I thank Mrs. Monique Wilhelm for giving me constant support throughout the course. I thank Ashley Cornet for teaching me RT-PCR, RNA isolation and cDNA synthesis. She is the one who first suggested I work in Dr. Sucic's lab. I would like to thank Larry Atherton for helping me order supplies and for setting up the new lab. I thank my friend Daniel Sherman, and his family for their love and support. From the first day I met him and till now, Dan was a good friend and his parents treated me as their own daughter. Also, I thank Jeremy Lynd and his family for their encouragement, not only for my thesis but also in my personal life. His parents and grandparents made me feel at home by treating me as one of their family members. I

thank all my friends- Ghada Sherif, Nickole Hatley, Nicole Soderberg, Soumya Pal, Tushar Ganjawala, Amanda Sheehy, Mary Christine Burger, Dr. Gerard Paez and my neighbors Ingrid, Wally, Bob, Greg, Diana and Mike Neithercut- for their love, care and encouragement. Lastly, I would like to thank University of Michigan-Flint College of Arts and Science and Office of Research for helping me in printing and binding my thesis.

Table of Contents

Abstract.....	ii
Acknowledgements.....	iv
List of Figures.....	vii
List of Tables.....	viii
Chapter 1: Introduction.....	1
Chapter 2: Materials and Methods.....	17
Chapter 3: Results.....	32
Chapter 4: Discussion.....	40
References.....	47
Appendices.....	53

List of Figures

Figure 1: Phases of a PCR reaction.....	14
Figure 2: Amplification of serially diluted DNA sample.....	15
Figure 3: A model of PCR program setup in Real-time PCR.....	22
Figure 4: Amplification plot.....	24
Figure 5: Melting curve.....	25
Figure 6: Postnatal developmental expression of widely expressed SPCs in the visual cortex of mice.....	36
Figure 7: Postnatal developmental expression of tissue-specific SPCs in the visual cortex of mice.....	37
Figure 8: Postnatal developmental expression of widely expressed SPCs in the visual cortex of mice during retinal degeneration.....	38
Figure 9: Postnatal developmental expression of tissue-specific SPCs in the visual cortex of mice during retinal degeneration.....	39

List of Tables

Table 1: Overall distribution of basic amino acid cleaving SPCs	9
Table 2: Cellular distribution of SPCs in rat brain	12
Table 3: The accession numbers of genes used for primer designing.....	19
Table 4: Sequence of upstream and downstream primers used in Real Time PCR.....	19
Table 5: Reaction for [cDNA] Optimization.....	21
Table 6: Temperature gradient used for annealing temperature optimization.....	26
Table 7: Combinations of upstream and downstream primer concentration.....	27
Table 8: Reaction mixture used for primer optimization.....	27
Table 9: Optimum parameters for SPC and GAPDH genes.....	27
Table 10: Regression analysis of standard curves for wt and rd mice at the early developmental time point.....	33
Table 11: Regression analysis of standard curves for wt and rd mice at the late developmental time point.....	33
Table 12: Results of correlation analysis showing the r values and significance levels of each gene.....	34

Chapter 1: Introduction

Brain Development and Plasticity

“There is no scientific study more vital to man than the study of his own brain. Our entire view of the universe depends on it.” - Francis H.C. Crick (*Scientific American*, September, 1979).

The brain is the most immature of all organs at birth and it continues to grow and develop after birth. The brain is composed entirely of two kinds of specialized cells: neurons and glial cells. Neurons are the basic information processing structures in the brain and glial cells provide assistance to the neurons by giving passive support, nourishment and removing wastes from the neurons (Temburni et al., 2001).

In most regions of the brain, no new neurons are formed after birth. Instead, brain development consists of an ongoing process of wiring and re-wiring the connections among neurons. Synapses are connections between neurons through which "information" flows from one neuron to another. New synapses between cells are constantly being formed, while others are broken or pruned away (Hawley, 2000).

Plasticity is defined as the ability of the brain to reorganize its connections structurally and functionally in response to changes in sensory experience. It is fundamental for the development of neuronal circuitry in central brain structures and for enabling the brain to adapt to its environment through changes in the sensory input (Tropea et al., 2009).

Visual Cortex

For our study we used the visual cortex of mice. The visual cortex is defined as the area of the occipital lobe of the cerebral cortex concerned with vision. The visual cortex has long been a proving ground for the study of experience-dependent plasticity, because visual experience can be easily manipulated and the consequences of manipulations can be readily measured at the anatomical, physiological, and molecular levels. The organization, development, and plasticity of the primary visual cortex represent an established model for studying the influence of neuronal activity on the organization of synaptic connections in the developing brain (Morino et al., 2003). Although the maturation of visual system circuitry starts before the onset of vision, proper development of the visual system requires sensory experience. In fact, the total absence of sensory input leads to a delay in the maturation of the visual cortex (Tropea et al., 2009). Visual experience increases the number and size of synapses per neuron as well as neuronal activity (Bengoetxea et al., 2008).

During postnatal development, the mouse primary visual cortex shows a gradual synaptic reorganization while cortical neurons (nerve cells that make the cortex of the brain) develop their adult, functional properties. Both structural and functional developments are activity-dependent. In active pathways, existing connections become strengthened and new ones are formed, whereas in inactive pathways connections are weakened and eliminated. The experience-dependent refinements of the neuronal connections are restricted to a short period, termed the critical period (Morino et al., 2003). Fagiolini et al. (1993) showed that the critical period begins around the end of the third postnatal week, peaks between the fourth and fifth week and starts to decline from

the end of the fifth week. During visual cortex development, a non-random relationship exists between the positions of neurons in the visual cortex and the retina. This wiring of neurons in a spatial organization is called the retinotopic map. Refinement of the retinotopic map takes place during the first week of life (before eye opening) (Cang et al., 2005). Later, when the retina receives visual stimuli, additional refinement and strengthening of the neural connections occurs.

For our study, wild type (wt) mice and retinal degeneration (Rd) mice were used. Wt mice ($Pde6b^{+}$) have normal vision. Rd mice ($Pde6b^{-}$) have a nonsense mutation in exon 7 of gene encoding the beta subunit of phosphodiesterase type 6 (Pde6b). Pde6b is found in the rod photoreceptors and it regulates the level of rod excitation in the presence and absence of light stimulation. During light stimulation rhodopsin is activated, which in turn activates transducin, a G-protein, by exchanging GDP for GTP. This leads to the activation of Pde6b, which then catalyzes the hydrolysis of cGMP to GMP and decreases the intracellular cGMP level. This decreased level of cGMP closes the cGMP gated Na^{+} ion channels and causes hyperpolarization of rod plasma membrane. This activates the photoreceptors and sends the signal to the retinal ganglion cells (RGC). RGC transmit signal from retina to several parts of the brain like thalamus and hypothalamus. The rd mice have a non functional Pde6b, which ultimately causes rod photoreceptor degeneration. So the signals are not sent to RGC, inturn to the brain. Mice homozygous for this mutation experience severe retinal degeneration.

Molecules Needed for Brain Development

Various molecules have been implicated as regulators or effectors of the physiological and structural modifications during critical periods for experience-dependent plasticity. These molecules are also needed for brain development. Among them, growth factors (including neurotrophins), neuropeptides, neurotransmitters and enzymes are vital for plasticity. For example, many secreted proteases play an important role in the degradation of extracellular matrix or cell surface proteins, or by the activation of specific membrane receptors by proteolysis (Morino et al., 2002). Also, vascular endothelial growth factor (VEGF) is the major angiogenic factor in the developing brain. VEGF also has neuroprotective and neurotrophic effects (Bengoetxea et al., 2008).

Neurotrophins

Neurotrophins are growth factors that play critical roles in the survival, differentiation, and the maintenance of the function of different neurons both in the peripheral and central nervous systems (CNS). In mammals, the neurotrophin family consists of four members:

1. Nerve- Growth Factor (NGF)
2. Brain-Derived Neurotrophic Factor (BDNF)
3. Neurotrophin-3 (NT-3)
4. Neurotrophin-4/5 (NT-4/5).

Their actions on neuronal tissue are mediated by two types of cell surface receptors:

- i) The high-affinity tyrosine kinase-related receptors (Trk family)
- ii) The low-affinity pan-NT receptor p75 (p75NTR), a member of the tumor necrosis factor receptor family.

The tyrosine kinase-related receptor family consists of three members. They are TrkA, TrkB and TrkC. NGF binds preferentially to TrkA, BDNF and NT-4 bind to TrkB, and NT-3 binds to TrkC. Specific binding of neurotrophins to their designated Trk receptors promotes neuronal survival, proliferation and differentiation, while the binding of neurotrophins to their common p75NTR, in the absence of Trk receptors, causes neuronal death (apoptosis) (Caleo et al., 2002).

Neurotrophins and Plasticity in Visual Cortex

Studies have indicated that neurotrophins might have an important role in the plasticity of the central nervous system in general and of the visual system in particular. The initial experiments started from the observation that neurotrophins and their receptors are present within the cortex (Pizzorusso et al., 2000). Later, it was shown that visual experience during development promotes the normal maturation of the visual cortex by regulating the production and uptake of neurotrophins. It is likely that visual experience during development acts as a gating process, promoting the expression of neurotrophin genes in the visual cortex, whose proteins strongly contribute to the refinement of visual neural connections (Pizzorusso et al., 2000).

Several studies on neurotrophin-receptor expression and their effects on visual cortical neurons or afferents to the visual cortex have indicated that different neurotrophins act on different neuronal targets (Berardi et al., 2003). For example, NT4, but not BDNF, regulates lateral geniculate nucleus soma size; BDNF, but not NGF, promotes GABA release in the visual cortex and regulates neuropeptide expression in interneurons (Wahle et al., 2003). Several observations have suggested that neurotrophins

control visual cortical plasticity during the critical period. Huang et al. (1998) showed that overexpression of BDNF in the visual cortex accelerates both the development of visual acuity and the time course of ocular dominance and synaptic plasticity, thus supporting a crucial role for neurotrophins in visual cortical development and plasticity (Berardi et al., 1999).

Neurotrophins and Apoptosis

When neurotrophins binds to their common p75NTR receptor they induce apoptosis. p75NTR is a receptor of the tumour necrosis receptor family, or cytokine receptor family. It activates ceramide production (a secondary messenger signaling molecule involved in apoptosis), nuclear factor k B (NF-kB) and C-Jun kinase (Chao et al., 1998). Pedraza et al. (2005) reported that, in the developing retina, cell death is caused by NGF/p75NTR interaction. NGF produced by microglia induces apoptosis in ganglion cells expressing p75NTR, with this effect being significantly reduced in a p75NTR knockout. It has also been demonstrated that oligodendrocytes, which normally express only p75, undergo rapid cell death in response to NGF. Suitable ectopic expression of TrkA in oligodendrocytes, obtained by retrovirus infection, rescues oligodendrocytes from death following NGF exposure (Pizzorusso et al., 2000).

Mature and Immature Forms of Neurotrophins

Neurotrophins are initially synthesized in a precursor form and their activation requires a cleavage at specific sites by prohormone convertase enzymes. While NGF and BDNF cause the neurons receiving them to survive, pro-NGF or pro-BDNF can induce

apoptosis (Pedraza et al., 2005). It has also been shown that pro-neurotrophins induces apoptosis through p75NTR. The pro-form of neurotrophins, which was considered an inactive form of the neurotrophin, has higher affinity for p75NTR and can induce apoptotic cell death even in the presence of Trk family receptors. The ability of p75NTR to induce cell death under mature NGF (mNGF) activation depends on the ratio of p75NTR/TrkA expression in a given cell model. So, the ratio of pro-NGF/mNGF and the ratio of p75NTR/TrkA plays a critical regulatory role for the maintenance of survival and death balance of neurons (Pedraza et al., 2005).

Subtilisin-like Proprotein Convertases (SPC)

Over the past few years a family of eukaryotic processing enzymes (called Subtilisin-like Proprotein Convertases, or SPCs, have been discovered that are evolutionarily related to the serine proteinases of the bacterial subtilisin family. Members of the SPC family have been characterized and shown to be responsible for the intracellular processing of many precursors at both single and clusters of basic residues (Seidah et al., 1994).

The mammalian SPCs constitute a family of nine serine proteinases. These include the seven basic amino acid- specific convertases known as PC1/3, PC2, furin, PC4, PACE4, PC5/6 and PC7 (Seidah and Chretien 1999; Zhou et al. 1999), and two proteinases that cleave at non-basic residues, namely subtilisin kexin isozyme 1/site 1 protease (SKI-1/S1P) (Sakai et al. 1998b; Seidah et al. 1999) and neural apoptosis-regulated convertase-1/proprotein convertase subtilisin-kexin like-9 (NARC-1/PCSK9) (Seidah et al. 2003; Benjannet et al. 2004). Of these, PACE4, PC4 and PC5 exhibit

multiple isoforms, most likely resulting from the generation of tissue-specific mRNAs by alternate splicing (Seidah et al. 2008). Some of the SPCs are expressed widely, while others are tissue specific.

These proteinases are implicated in the limited proteolysis of precursors of secretory proteins that participate in several biological functions, such as development, reproduction and immune response, and in numerous pathologies (Seidah et al. 1999). The SPCs are implicated in the processing of multiple protein precursors like propeptide hormones, neuropeptides, growth factors, receptors, adhesion molecules, enzymes, clotting factors, blood proteins and proteins of extracellular matrix. SPCs have also been linked to various pathologies such as Alzheimer's disease, tumorigenesis, and infections. In Alzheimer's disease, furin and PC5 were found to process the zymogens of both α - and β -secretase. β -secretase is involved in the generation of β -amyloid, the principal component of senile plaques in Alzheimer's disease. SPCs are involved in processing and activation of various molecules involved in tumorigenesis and metastasis. These include metalloproteases, adhesion molecules, growth factors, and growth factor receptors. They are also involved in activation of various bacterial toxins like Diphtheria toxin, *Pseudomonas aeruginosa* exotoxin A (PEA), Botulinum neurotoxin and *Bordetella* dermonecrotic toxin. They also activate various viral glycoproteins like gp160 of HIV, influenza virus hemagglutinins, and Ebola virus glycoproteins (Scamuffa et al., 2006).

Basic Amino Acid- Specific Convertases: Widely Expressed Members

Furin is ubiquitously expressed and is primarily localized in the *trans*-Golgi network (TGN), but also cycles to the cell surface. Furin processes precursors generated

in constitutively secreting cells, and usually cleaves substrates at the consensus type I cleavage site N-Arg-Xaa-(Lys/Arg)-Arg-C. PACE4, and to a lesser extent PC5. are distributed in some endocrine and non-endocrine cells (Seidah., 1996). The mRNA for PACE4E is expressed in various region of brain, such as the olfactory bulb, cerebral cortex, hippocampus, and cerebellum (Akamatsu et al 1997). PC7 transcripts are also widely expressed at high levels in the brain. PACE4 and PC7 are expressed and function ubiquitously within the constitutive secretory pathway (Tsuji et al., 1994). The tissue distribution and intracellular localization of basic amino acid cleaving SPCs are given table 1.

Basic Amino Acid- Specific Convertases: Tissue Specific Members

PC1/PC3 and PC2 are the major forms expressed in the neuroendocrine system and brain, where they act on prohormone and neuropeptide precursors in the regulated secretory pathway. PC1 and PC2 are localized within the TGN and in dense-core secretory granules. PC4 is exclusively expressed in testicular germ cells (Seidah., 1996).

Non Basic Amino Acid- Specific Convertases

NARC-1/PCSK9 is a proprotein convertase that plays a major role in cholesterol homeostasis through enhanced degradation of the low density lipoprotein receptor (LDLR). Because of the importance of cholesterol in synaptogenesis (described below), PCSK9 must also be involved in neural development. PCSK9 is only transiently expressed in cortical cells of the kidney and in specific brain regions where active neurogenesis takes place (Poirier et al., 2006).

Name	Tissue distribution	Intracellular Localization
Furin	Ubiquitous, but expressed at variable levels	TGN, endosomes and cell surface
PC2	Neuroendocrine cells	Secretory granules
PC1	Neuroendocrine cells	Secretory granules, TGN
PACE4	Endocrine and non endocrine cells, widespread tissue expression	Primarily extracellular
PC4	Testicular germ cells	Not Known
PC5- A	Endocrine and non endocrine cells, widespread tissue expression	Primarily extracellular
PC5-B	Digestive system and adrenal cortex	TGN
PC7	Widespread, with high level in lymphoid-associated tissue	TGN

Table 1: Overall distribution of basic amino acid cleaving SPCs (Bergeron et al, 2000)

SPCs and Neurotrophins

Some of the SPC's are expressed in neurons and glial cells, but some SPCs are expressed only in neurons (Table 2). Neurotrophins are produced both by constitutively secreting cells (e.g. fibroblasts and glial cells) and in cells containing dense core secretory granules (e.g. granular tubule cells in mouse mandibular glands, neurons, and mast cells). It has been demonstrated that proNGF could be processed intracellularly in both constitutive and regulated cells. Bresnahan et al. (1990) showed that yeast kexin and human furin are capable of processing mouse proNGF to NGF. Other results confirmed that furin, and to a lesser extent PACE4 and PC5, are the best candidates for proNGF convertases (Seidah et al., 1996). Hippocampal neurons and AtT-20 cells in culture process NGF within the constitutive secretory pathway. Constitutive release of NGF

occurs soon after the molecule is synthesized. Thus, as a result of being processed in the constitutive pathway, NGF is continuously available to cells that require it (Farhadi et al., 2000).

proBDNF and proNT3 can be processed by furin and, to a lesser extent, PACE4 and PC5 (Seidah et al., 1996). Furthermore, human proNT3 is sulfated, suggesting that processing of proNT3 occurs following the arrival of the precursor to the TGN (Seidah et al., 1996). In contrast to NGF, hippocampal neurons process BDNF within the regulated secretory pathway. Intact pro-BDNF can be shunted from the TGN into immature secretory granules where it is likely cleaved by PC1. BDNF is stored within dense core vesicles, and once released, presumably in response to extracellular cues, it can induce changes in neuronal structure, membrane depolarization, and synaptic function. NT-3 is primarily processed by furin-like enzymes and released constitutively. NT-3 may regulate neuronal depolarization and synaptic plasticity, but as yet little is known about its intracellular sorting *in vivo* (Farhadi et al., 2000).

In contrast to the mature forms, the unprocessed forms of neurotrophins bind with high affinity to the p75NTR receptor along with a co-receptor called sortilin. Sortilin (95 kDa) is a member of Vps10p-domain receptor family and is expressed in a variety of tissues, notably brain, spinal cord and muscle (Nykjaer et al., 2004). Recent studies have shown that the unprocessed precursor form of neurotrophin family members, such as proNGF and proBDNF, can act through a co-receptor system of p75NTR and sortilin to mediate cell apoptosis. Thus, SPCs may likely play a vital role in visual cortex development and plasticity by processing some important neurotrophins, growth factors

and neuropeptides. However, little is known about the expression of SPC's during the development of visual cortex.

SPC	Neuron	Glial
Furin	+	+
PC2	+	
PC1	+	-
PACE4	+	+
PC5	+	
PC7	+	+

Table 2: Cellular distribution of SPCs in rat brain (Bergeron et al, 2000)

Cholesterol and Synapse Formation

Cholesterol is needed by neurons to form synapses, as it is required to activate a signaling pathway that triggers synaptogenesis. Also, a sufficient amount of cholesterol itself might be needed to support the structural demands of synaptogenesis. For example, cholesterol binds to several synaptic proteins, and is necessary for the formation of synaptic vesicles and for the clustering of certain postsynaptic receptors. Studies have reported that the source of cholesterol for fetal and postnatal development is newly synthesized cholesterol (Hanaka et al., 2000). This cholesterol is synthesized by astrocytes and it is taken up by neurons through receptor mediated endocytosis (Barres et al., 2001).

The low density lipoprotein receptor and very-low-density-lipoprotein (VLDL receptor) are both members of the LDL receptor family that play roles in the uptake of cholesterol and triglyceride rich lipoproteins, respectively. LDLR binds apo-B-100 and

apo E-containing lipoproteins. On the other hand, VLDL receptor binds only apo E-containing lipoprotein. Both receptors are expressed in the brain (Hanaka et al., 2000). LDLR helps in the uptake of cholesterol rich lipoproteins by endocytosis. Once the LDL protein is released, LDLR is recycled to the cell surface for binding to another LDL protein. The LDL receptor-related protein (LRP) also helps in the uptake of cholesterol and has also been directly implicated in synaptic plasticity in hippocampal slices (Barres et al., 2001). PCSK9 is also expressed in brain and it plays a very important role in regulating cholesterol uptake by degrading LDLR. PCSK9 is secreted into the plasma environment, where it either exists in free form or may become associated with plasma LDL. PCSK9 binds to LDLR and causes LDLR mediated endocytosis which results in delivery of both LDLR and PCSK9 to endosomal/ lysosomal compartments. Here, the LDLR is degraded and is not recycled to the cell surface. PCSK9 regulates the uptake of cholesterol by regulating degradation of the LDLR (Qian et al., 2007). Hence, PCSK9 might be important in visual cortex development.

End Point PCR vs. Real Time PCR

Polymerase Chain Reaction (PCR) is used to amplify a specific DNA sequence into many copies. Real-time PCR amplifies a specific target sequence in a sample then monitors the amplification progress using fluorescent technology (Valasek and Repa, 2005). A basic PCR run can be broken up into three phases (Figure 1):

Exponential: Exact doubling of product is accumulating at every cycle (assuming 100% reaction efficiency). The reaction is very specific and precise.

Linear (High Variability): The reaction components are being consumed, the reaction is slowing.

Plateau (End-Point): The reaction has stopped, no more products are being made, and, if left long enough, the PCR products will begin to degrade.

End point PCR detects the product at the plateau phase and real-time PCR detects the product during the exponential phase (Mark et al., 2005). Since RT-PCR can detect the product at exponential phase, it actually reflects the amount of target DNA present before any amplification (Figure 2). With end point PCR, there may be different amounts of target DNA at the start of the reaction, but at the plateau phase the same amount of product may be produced (Mark et al., 2005)

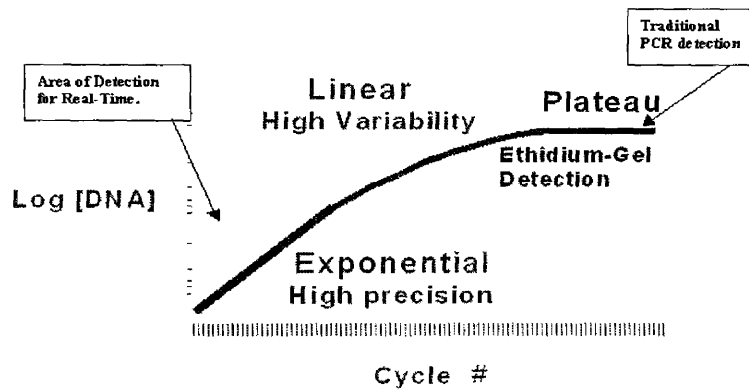


Figure 1: Phases of a PCR reaction. Graph showing three phases of a PCR reaction – exponential phase, linear phase and plateau phase. Real-Time PCR detects the product at exponential phase, while end point PCR detects the product at plateau phase.

Real-Time PCR provides fast, precise and accurate results. It can detect as little as 5 copies of target DNA. Real-Time PCR is designed to collect data as the reaction is

proceeding, which is more accurate for DNA and RNA quantification and does not require laborious post PCR methods (Dieter Klein, 2002).

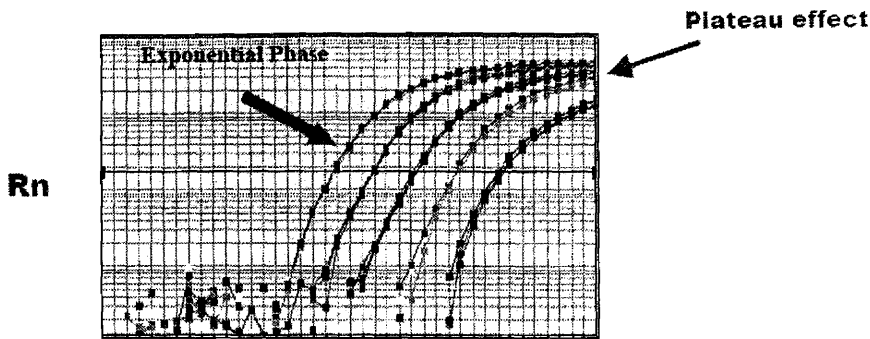


Figure 2: Amplification of serially diluted DNA sample. The 5-fold dilution series of DNA show the same accumulation of product at plateau phase, even though the exponential phase clearly shows a difference between the points along the dilution series. This reinforces the fact that if measurements were taken at the plateau phase, the data would not truly represent the initial amounts of starting target material.

SYBR Green

RT-PCR uses fluorescent dyes to measure the DNA amplification. The dye that we used in our study was SYBR green I. It binds to the minor groove of double-stranded DNA (dsDNA) and emits 1,000-fold greater fluorescence than when it is free in solution. Therefore, the greater the amount of dsDNA present in the reaction tube, the greater the amount of DNA binding and fluorescent signal from SYBR green I (Valasek and Repa, 2005).

Real time data can be quantified absolutely and relatively (Yuan et al., 2006). In our study, a relative quantification method was used to study changes in gene expression by measuring changes in expression of a gene of interest relative to an invariant control gene (reference gene). Housekeeping genes (e.g., cyclophilin, glyceraldehyde-3-

phosphate dehydrogenase (GAPDH), ribosomal protein 36B4, β -actin, 18S rRNA, transferrin receptor, etc.) that are not expected to change under the experimental conditions serve as a convenient internal standard (Pfaffl et al., 2001). In our study we used GAPDH as a reference gene. (The relative quantification method is discussed in detail later).

Our Study

SPCs may play an important role in development of the visual cortex by processing neurotrophins and neuropeptides, and by helping in cholesterol homeostasis. However, little is known about the expression and role of SPC's during brain development. We studied the expression of SPC's in the visual cortex of wt and rd mice during postnatal development. To study the expression of different SPCs at the mRNA level, we used quantitative Real Time PCR because it is accurate, fast and precise. Understanding the expression of SPCs during development of the visual cortex will form the basis for understanding the function of SPCs in brain development, which is not yet well characterized. Comparing the expression of SPCs during the development of the visual cortex in wt and rd mice could allow for understanding the potential role of SPCs in neurodegenerative diseases. and finally may lead to find the therapeutic treatment for such diseases.

Chapter 2: Materials and Methods

Obtaining Visual Cortex of Mice:

Visual cortex tissue from mice (wt and rd) at ten different time points (postnatal week 1, week 2, week 3, week 4, week 5, week 6, week 7, week 14, week 21 and week 35) was isolated by Dr. Jarvinen. As soon as the tissue was isolated, it was suspended in the pre-chilled lysis buffer provided by Invitrogen (Carlsbad, CA). The dissection of visual cortex was done on ice and the RNA was isolated immediately to avoid any degradation of RNA.

RNA Extraction

The RNA from the brain tissue was extracted using the PureLink™ Micro-to-Midi Total RNA Purification System (Invitrogen) as instructed by the manufacture. The RNA sample was stored at -80°C for future use.

DNase Treatment

The RNA sample was treated with DNase to degrade any genomic DNA contamination. RNA was incubated with DNase I, Amplification Grade (Invitrogen), for 15 minutes at room temperature and the enzyme was inactivated by adding 25mM EDTA and incubating at 60°C for ten minutes. The DNased RNA was stored at -80°C.

cDNA Synthesis

cDNA was synthesized from every DNAsed RNA sample using Superscript™ III First-Strand Synthesis System for RT-PCR, as instructed by the manufacture (Invitrogen). cDNA synthesis without adding the reverse transcriptase was used as a negative control (called pseudo-cDNA) to check for contamination of the reagents.

PCR Reaction

The presence of cDNA in the DNAsed cDNA sample and the absence of contamination in the pseudo-cDNA sample were verified by amplifying GAPDH. The amplified PCR product was subjected to 1% agarose gel electrophoresis in 0.5x TBE buffer for 1 hour at 90 volts. The gel was stained with ethidium bromide, destained in tap water, and visualized under UV. The expected PCR product length was 561 bp. The presence of a DNA band of 561 bp length in the original sample and the absence of the band in the pseudo-cDNA sample confirmed that cDNA could be used for Real-time PCR.

Real-Time PCR

Primer Designing

The sequences of mouse GAPDH, furin, PACE4, PC1, PC2, PC5A, PC7 and PCSK9 were obtained from GenBank (www.ncbi.nlm.nih.gov/Genbank). The accession numbers for these genes are given in the Table 3. The primers (upstream and downstream) were designed using LaserGene Software (DNASTAR; Madison, WI). The

primers were designed such that the size of the PCR product was between 100-200 base pairs. The sequence of the primers and respective product length is shown in Table 4.

Gene	Accession number
GAPDH	XR_031086.1
Furin	NM_001081454.1
PACE4	XM_886136.2
PC1	NM_013628.2
PC2	NM_008792.3
PC5	XM_129214.6
PC7	NM_008794.2
PCSK9	NM_153565.1

Table 3: the accession numbers of the genes used for primer designing and real-time PCR

Gene	Sequence of primers	Size of the PCR product
Furin	Up- 5'-GAAAATACCAGTGAAGCCAACAAC-3' (2045-2068) Down-5'-AGGCCTGGCTGGATGTGA-3' (2160-2177)	133
PACE4	Up- 5'-CTGTCTTGTCGCCGTGGGTCTAT-3' (274-297) Down-5'-ACACAGTGCACCTTCTCAGGTTTCAT-3' (407-430)	157
PC1	Up- 5'-TTGGCTGAAAGGGAAAGAGATACA-3' (1681-1704) Down-5'-TGTCCCATGCAAAATCAA-3' (1840-1857)	177
PC2	Up- 5'-CAACGCGACCAGGAGAGGAGACC-3'(1849-1871) Down-5'-GGTCCCTCGGGCATCCTC-3' (1994-2011)	163
PC5	Up 5'-ACCTCAGCCATGCCCAGTCAACC- 3' (986-1008) Down 5'-CGATATTCTTCCCCGTGTAGC-3' (1112-1132)	147
PC7	Up- 5'-GCCCCATGCTGAAAGAAAATAAGG-3' (1645-1668) Down-5'-AGACATCATGCCACTGGGACAAAA-3'(1815-1838)	194
PCSK9	Up- 5'-GCGTCCAAAATTAGTCCCCAAAGT-3' (1800-1821) Down-5'-AGGACTGGGGTGGTGCTGGTTGC-3' (1945-1964)	156
GAPDH	Up- 5'-GGCAAGGTCATCCCAGAGC-3' (704-722) Down-5'-CCTTCAGTGGGCCCTCAGATGC-3' (845-866)	163

Table 4: Sequence of upstream and downstream primers for each gene for real-time PCR, the nucleotide position of the primers, and the respective product size of each primer.

Sequencing of Real-Time PCR Products:

Each primer set was used to make a PCR product. The product was cloned into pCR®4-TOPO vector by Nickole Hatley and Dr. Ann Sturtevant using the TOPO TA Cloning® Kit for sequencing (Invitrogen), as directed by manufacture's instructions.

The PCR constructs were transformed into *E.coli* XL1-Blue competent cells and plated onto LB-ampicillin agar (200µg/ml ampicillin) using standard protocols as directed by "Molecular Cloning: A Laboratory Manual" (Sambrook and Russell, 2001). The following day, the colonies on the LB-ampicillin plates were cultured in separate 5 ml LB broth tubes containing 200mg/ml ampicillin and incubated overnight at 37°C.

The next day, small scale plasmid purification was done for each sample using QIAprep® Spin Miniprep Kit (QIAGEN; Valencia, CA) as directed by the manufacture's instructions. The plasmids were digested with EcoR1 and checked for the presence of PCR product. The samples were sent to the DNA Sequencing Core at the University of Michigan – Ann Arbor. After obtaining the sequence results, BLAST was performed to confirm that the sequence obtained was the desired PCR product.

Real Time PCR Using QuantiFast SYBR Green

Overview and Background Calibration

For any PCR reaction, the conditions should be optimized. Even for real-time PCR, certain conditions like cDNA concentration, annealing temperature, and primer concentration have to be optimized to obtain the right PCR product and maximal efficiency. The optimum parameters used for each gene are shown in Table 9. SYBR

Green normally has some background fluorescence, so background calibration was done using the plates provided by the manufacturer (Mastercycler® ep realplex, Eppendorf).

cDNA Concentration Optimization

The concentration of the cDNA used for the real-time PCR was optimized as suggested by Table 1 of QuantiFast SYBR Green PCR Handbook 01/2007 (QIAGEN). Optimizing the cDNA concentration can prevent non-specific PCR product formation. Furthermore, less concentration of cDNA can be used, hence saving cDNA. The reaction setup for cDNA concentration optimization was done as shown in Table 5.

Reaction Components	Variation 1	Variation 2	Variation 3	Variation 4
[cDNA]	2.5 µl [1:4]	1 µl [1:4]	2.5 µl [1:10]	1 µl [1:10]
SYBR Green	12.5 µl	12.5 µl	12.5 µl	12.5 µl
Up stream primer [25µM]	1 µl	1 µl	1 µl	1 µl
Down stream primer [25µM]	1 µl	1 µl	1 µl	1 µl
RNase free water	8 µl	9.5 µl	8 µl	9.5 µl
Total	25 µl	25 µl	25 µl	25 µl

Table 5: Reaction components for cDNA concentration optimization

Before starting each PCR reaction, the plate layout and the PCR program for the reaction were set up in the computer and saved as directed by the Mastercycler ep *Realplex*⁴ software manual (Eppendorf). A model of the PCR program was shown in Figure 3.

All the PCR reactions were set up in an ice box to prevent primer dimer formation and to keep the reagents non-reactive. The reaction set up was done in a Labconco PCR hood to prevent contamination. SYBR Green master mix was always half the total

volume of the reaction and the total reaction volume was 25 μ l. Two concentrations of cDNA (1:4 and 1:10) and two different volumes (1 μ l and 2.5 μ l) were used. cDNA amount did not exceed 10% of the final volume. Then, 1 μ l of 25 μ M upstream and downstream primers were added so that the final concentration of the primer was 1 μ M. Finally, RNase free water was added to adjust the volume to 25 μ l. No Template Control (NTC), which contained all the reagents and RNase free water instead of cDNA, was also done to check for contamination in the reagents. All the reactions were done in triplicates to check the reproducibility of the reaction and to avoid any bias.

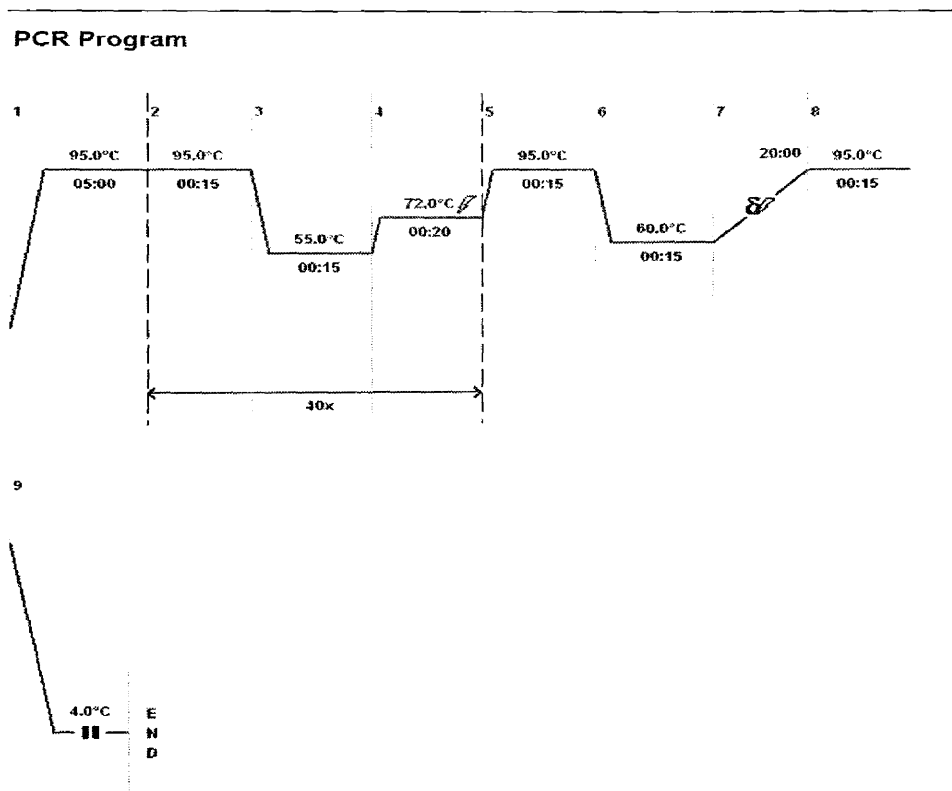


Figure 3: PCR program used for [cDNA] optimization. Initially, the program was set for 95⁰C for 5 minutes to activate *Taq* polymerase. The PCR cycles were programmed for denaturation at 95⁰C for 15 seconds, annealing at 55⁰C for 15 seconds and extension at 72⁰C for 20 seconds; this was repeated for 40 cycles. After the PCR reaction, the product was subjected to melting curve analysis.

After the reaction set up, clear cap strips were placed on the wells and the wells were closed tightly. The plate was centrifuged for 15 seconds at 3000 rpm to mix the reagents and to avoid air bubbles in the reaction tube. The plate was then placed in the Mastercycler *Realplex⁴*, the strips were wiped off with lint-free cloth, the lid of the machine was closed and the PCR program was started. For each real-time PCR reaction, the software generated two different types of plot: an Amplification plot and a Melting curve

Amplification Plot

SYBR green binds to dsDNA and gives off fluorescence. During the PCR reaction, a particular gene product gets amplified and the amount of double stranded DNA (ds DNA) increases, causing the fluorescence to increase. At the end of each cycle the detector reads the fluorescence and plots it against the cycle number. This is called an amplification plot. This plot has three phases: exponential phase, linear phase and plateau phase, as described in the Introduction. Real-time PCR allows for detection of the product at exponential phase.

The amount of fluorescence is associated with the amount of PCR product. The amount of PCR product depends upon the original amount of target cDNA added to the reaction. The amount of cDNA reflects the amount of mRNA transcripts in the lysates of visual cortex tissue. Thus,

More fluorescence → more PCR product → more cDNA → more mRNA transcript

Each amplification plot has a threshold level calculated by the software. The default setting, called the Noise Band, was used for all the reactions, where the threshold

level was calculated to be 10 standard deviations above the Noise Band. The cycle at which the fluorescence signal of any sample crosses the threshold was called the Ct (Cycle threshold) value of the sample. The three phases of PCR reaction, threshold level and Ct are shown in Figure 4.

During amplification, the time required for the fluorescent signal to reach a Ct correlates with the amount of original target sequence. In other words, the Ct value is inversely proportional to the amount of specific nucleic acid sequence in the original sample. A lower Ct value means the reaction was more efficient, which in turn means that there was more cDNA to start with (the more cDNA we have, the less cycles it takes for the fluorescence to cross the threshold). Thus,

Low Ct → more PCR product → more cDNA → more mRNA transcript

The cDNA concentration that has the lowest Ct value and is highly reproducible was chosen as the optimum cDNA concentration.

Amplification Plot

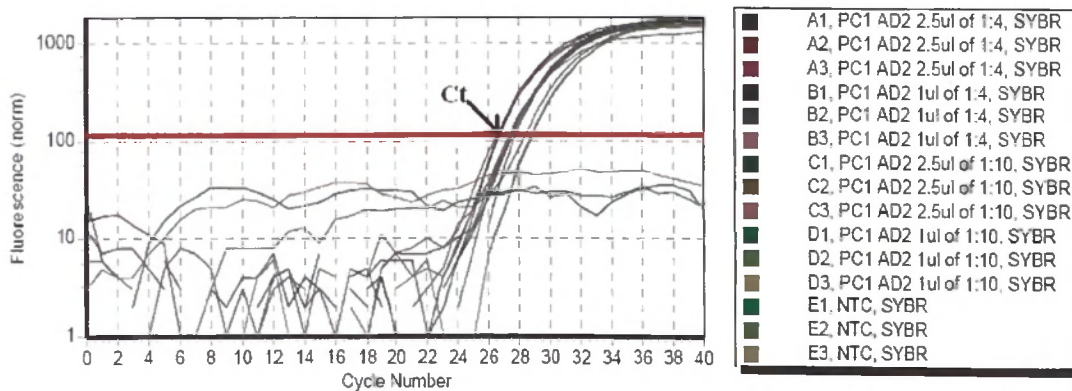


Figure 4: Amplification plot. Amplification plot showing the threshold level (red line), noiseband, the amplification curve and the Ct value.

Melting Curve

For an optimal PCR reaction the Ct value should not only be low, but also a proper melting curve is necessary. SYBR Green is not sequence specific. It binds to any double stranded DNA, including primer dimers. After each PCR reaction, the PCR products can be analyzed through a melting curve. For this, samples are subjected to increasing temperature. The temperature at which each product melts depends on its length and nucleotide composition (GC content). The software generates the melting curve by plotting a dissociation curve of the product DNA against temperature (Figure 5). The melting curve shows a spike indicating the temperature at which the product melts. A single peak indicates that there is only one PCR product. If there is more than one peak, then there are non specific amplification products or primer dimers. For a valid real-time PCR reaction, the Ct value should be low and reproducible, and the melting curve should have a single peak.

Melting curve

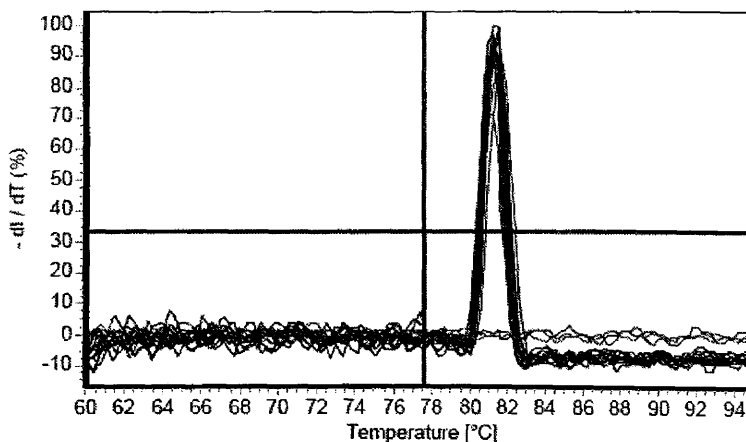


Figure 5: Melting curve. Melting curve showing the temperature at which the amplified DNA product dissociates.

Annealing Temperature Optimization

Annealing temperature optimization was done for each gene according to “Optimization of the new Lambda Primers-Gradient PCR” (Eppendorf). The optimum cDNA concentration was used for annealing temperature optimization. A temperature gradient was set up across the 12 columns of the plate (Table 6) to vary the annealing temperature and all other steps of the program were the same. The reaction mixture contained the optimum concentration of cDNA, 1 μ l of 25 μ M upstream primer and 1 μ l of 25 μ M downstream primer, 12.5 μ l of SYBR Green master mix, with the final volume made up to 25 μ l using RNase free water. All the reactions were done in triplicate with one NTC for each temperature. The annealing temperature that gave the lowest Ct and was highly reproducible was chosen for each gene and used for subsequent analysis.

Column in 96 well PCR plate	1	2	3	4	5	6	7	8	9	10	11	12
Annealing temperature in $^{\circ}$ C	50.0	50.2	50.8	51.7	52.8	54.1	55.4	56.7	57.9	58.8	59.5	59.9

Table 6: The gradient temperature used for annealing temperature optimization for all SPC genes and GAPDH gene.

Primer Concentration Optimization

Primer concentrations were optimized according to “Optimization of the new Lambda Primers-Gradient PCR” (Eppendorf). A combination of three different concentrations of upstream primer and downstream primers were used (Table 7). They were 6.25 μ M, 12.5 μ M and 25 μ M concentrations and they result in a final concentration of 250 nM, 500 nM and 1000 nM, respectively, in a 25 μ M reaction volume. The reaction

components are shown in Table 8. All reactions were done in triplicate with NTC. The primer combination that gave the lowest Ct with high reproducibility was chosen.

		Downstream primer concentration		
		250nM	500nM	1000nM
Upstream primer concentration	250nM	250/250	250/500	250/1000
	500nM	500/250	500/500	500/1000
	1000nM	1000/250	1000/500	1000/1000

Table 7: Different combinations of upstream and downstream primer concentrations used in primer optimization for all genes.

Reaction Components	Volume
cDNA	1 μ l [1:4]/[1:10]
SYBR Green	12.5 μ l
Upstream primer	1 μ l (6.25 μ M, 12.5 μ M or 25 μ M)
Downstream primer	1 μ l (6.25 μ M, 12.5 μ M or 25 μ M)
RNase free water	9.5 μ l
Total	25 μ l

Table 8: Real-time PCR reaction components: All the components were same for all the reactions except the primer concentration.

Gene	[cDNA]	Annealing temperature in $^{\circ}$ C	[Primer] Up/Down
Furin	1 μ l [1:4]	63.3	500nM/1000nM
PACE4	1 μ l [1:4]	53.8	1000nM /1000nM
PC1	1 μ l [1:4]	50.2	500nM /500nM
PC2	1 μ l [1:10]	56.7	500nM /500nM
PC5A	1 μ l [1:4]	55.4	1000nM /500nM
PC7	1 μ l [1:4]	51.7	250nM /500nM
PCSK9	1 μ l [1:4]	59.5	500nM /1000nM
GAPDH	1 μ l [1:4]	56.5	1000nM /1000nM

Table 9: Optimum [cNDA], annealing temperature and [primer] for each gene.

Standard and Efficiency Curves

Standard curves were generated to determine the efficiency of the PCR reaction. To do each standard curve, five 10-fold serial dilutions of cDNA were prepared from

undiluted cDNA (1x) and real-time PCR was done in triplicate for each dilution using optimum parameters. The computer software creates the standard curve by plotting Ct value vs $\text{Log}_2[\text{cDNA}]$. The efficiency of the reaction was calculated from this curve (Yuan et al., 2006). In a PCR reaction, theoretically, the number of PCR products should double in each amplification cycle, so the percentage of amplification efficiency (PAE) should be 100%. This would be equal to the amplification efficiency (AE) of 2, which is calculated by 2^{PAE} . This means that at each cycle the number of product molecule is doubling (Yuan et al., 2007). Practically, the AE for a PCR reaction may not be exactly 2 depending on number of criteria like [primer], annealing temperature, pipetting error and experimental error.

In our study, if the PAE of wt and rd reactions were different, it would be a problem and the results of subsequent analyses would not be reliable. To determine the PAE, standard curves were done for four different samples (one wt and rd from an early developmental time point and one wt and rd from a late developmental time point) and PAE was calculated. The regression line should have the slope of -1, where $\text{PAE} = -(\text{slope})$. The line should also show a high R^2 value. In our study, two criteria were used

- i) The slope of the standard curve should not be significantly different from -1
- ii) The slope of wt and rd should not be significantly different from each other.

If these two criteria were met, then the PAE value was accepted. If the criteria were not met, the value of PAE was used as a correction factor (Yuan et al., 2007).

For standard curve analysis, all the reactions were done in triplicate for each dilution and the three Ct values were obtained. The two closest Ct values were used for the analysis. The mean of the two Ct values was taken, resulting in one Ct for each dilution.

These data were analyzed using SPSS by simple linear regression models and 95% confidence intervals. The data and syntax for standard curve analysis are shown in Appendix 1, 2 and 3. The standard curve was done for each gene and the data were analyzed. If the slope of wt and rd were significantly different, then the correction factor was used in subsequent analysis.

Real-Time PCR for Individual Samples

All cDNA samples from wt and rd mice were subjected to real-time PCR using the optimum [cDNA], annealing temperature and [primer] for each gene. All the reactions were done in triplicate along with NTC. The Ct values were collected and used for analysis

Data Analysis Criteria

Three Ct values were obtained. For data analysis only the two closest Ct values were used. The two closest Ct values should be within one amplification cycle. If this criterion was met, the two Ct values were segregated into high and low Ct values (Appendix 4). If the criterion was not met, then the PCR reaction was repeated in triplicate and the two closest Ct values that were within one amplification cycle were used.

Correlation Analysis

The high and low Ct values were collected for all samples and for all genes. Then, correlation analysis was performed between same age and genotype. We expected that the Ct values would be similar for all animals of the same genotype at the same age for the same gene. The syntax used for correlation is shown in Appendix 5.

$\Delta\Delta\text{Ct}$ Method

The mean of the accepted duplicates was used for gene expression analysis. $\Delta\Delta\text{Ct}$, a relative quantification method, was used (Yuan et al., 2007). The analysis was divided into two parts.

i) First, the expression of SPC genes during the normal development of visual cortex in wt mice was analyzed. The ΔCt value for each gene was calculated by subtracting the high Ct of GAPDH from the high Ct of target gene and the low Ct of GAPDH from the low Ct of target gene at each age (Equation 1)

$$\Delta\text{Ct} = \text{Ct}_{\text{Target}} - \text{Ct}_{\text{GAPDH}} \quad (1)$$

To calculate $\Delta\Delta\text{Ct}$, the ΔCt data points for each age were ordered from highest to lowest in value. The highest ΔCt value for each age was subtracted from the highest week 35 ΔCt value and the lowest ΔCt value for each age was subtracted from the lowest week 35 ΔCt value, because the week 35 mice were considered to be adult age (Equation 2). The $\Delta\Delta\text{Ct}$ values are shown in Appendix 6.

$$\Delta\Delta\text{Ct} = \Delta\text{Ct}_{\text{targetPND250}} - \Delta\text{Ct}_{\text{targetPND7}} \quad (2)$$

Differences in the expression of each gene in the developing visual cortex were evaluated by separate one-way ANOVAs, with Age as the between-subject variable.

ii) In the second analysis, differences in expression of SPC genes in the diseased visual cortex were evaluated. The ΔCt value for each gene was calculated by subtracting the high Ct of GAPDH from the high Ct of target gene and the low Ct of GAPDH from the low Ct of target gene at each age (Equation 1). To calculate the $\Delta\Delta\text{Ct}$ value for each gene, the highest ΔCt of rd was subtracted from the highest ΔCt of wt and the lowest ΔCt

of rd was subtracted from the lowest ΔCt of wt for each gene at each age (Equation 3).

The $\Delta\Delta\text{Ct}$ values are shown in Appendix 7.

$$\Delta\Delta\text{Ct} = \Delta\text{Ct}_{\text{wt}} - \Delta\text{Ct}_{\text{rd}} \quad (3)$$

Two-way ANOVA with Genotype and Age as between-subject variables was done using SPSS software. In all statistical analyses, post-hoc pairwise comparisons using a conservative Bonferroni adjustment were done to determine significant differences between means, with $p < .05$ considered statistically significant (Appendix 8).

Chapter 3: Results

Standard and Efficiency Curve Analysis

The standard and efficiency curves were tested using simple linear regression analysis. The standard curve was performed at two different time points: one wt and rd from an early developmental time point and one wt and rd from a late developmental time point. The expected results were that the slope of the standard curve should not be significantly different from -1 and the slope of wt and rd mice should not be different from each other. The regression analysis showed that the slope of wt mice was not significantly different from the slope of rd mice at both time points ($P > 0.05$) (Table 10 and 11). The regression analysis showed that the lines were not significantly different from -1 for the wt and rd mice at both time points for all genes, except for PC1 at the early time point and furin at the late time point (Table 10 and 11). Although the slopes of the PC1 and furin standard curves were significantly different from -1, PAE was not used for subsequent analysis because of the small sample size, as discussed later. The standard curve for PCSK9 was not generated because the Ct values obtained with undiluted cDNA were quite high, which means the expression of PCSK9 was very low; there was no amplification of PCSK9 from any diluted cDNA.

Correlation Analysis

Correlation analysis was done for all Ct values. We predicted that the Ct values would be similar for all animals of the same genotype at the same age for the same gene. The correlation result showed that the Ct values were in fact highly correlated for animals

of the same age, same genotype, and same gene. The r values were high and showed significant correlation at 0.01 levels, except for GAPDH, PACE4 and PC2 at week 3, for which the correlation was significant at 0.05 level, and GAPDH at week 6, which was marginally significant (P=0.126) (Table 12).

Gene	Wt mice	Rd mice	P value
GAPDH	-1.114	-1.099	0.836
Furin	-0.976	-0.915	0.567
PACE4	-1.080	-1.138	0.735
PC1	-0.929	-0.907	0.534
PC2	-1.152	-0.996	0.666
PC5	-1.045	-0.918	0.459
PC7	-1.392	-1.293	0.775

Table 10: Regression analysis of standard curves for wt and rd mice at the early developmental time point. Slopes and P values from regression analysis of wt and rd mice for each gene at the early time point are given here. The slopes of wt and rd mice were not significantly different from each other (P>0.05). Also, the slopes of wt and rd mice were not significantly different from -1, except for PC1 (shown in bold).

Gene	Wt mice	Rd mice	P value
GAPDH	-0.989	-1.051	0.408
Furin	-0.844	-0.798	0.466
PACE4	-1.155	-1.175	0.953
PC1	-0.909	-0.949	0.885
PC2	-0.855	-0.870	0.940
PC5	-1.103	-0.920	0.226
PC7	-1.130	-1.045	0.456

Table 11: Regression analysis of standard curves for wt and rd mice at the late developmental time point. Slopes and P values from regression analysis of wt and rd mice for each gene at the late time point are given. The slopes of wt and rd mice were not significantly different from each other (P>0.05). Also, the slopes of wt and rd mice were not significantly different from -1 except for furin (shown in bold).

ΔΔCt Analysis Using Post-hoc Pairwise Comparisons

ΔΔCt analyses were performed to compare the expression of SPCs during normal postnatal developmental of the visual cortex in wt mice. These analyses were also used to compare the expression of SPCs in rd mice during retinal degeneration.

Age	Genes							
	GAPDH	Furin	PACE4	PC1	PC2	PC5A	PC7	PCSK9
Week 1	.994	.997	.995	.992	.996	.998	.997	.993
Week 2	.981	.997	.973	.963	.900	.887	.995	.963
Week 3	.893*	.995	.879*	.957	.908*	.989	.984	.940
Week 4	.985	.958	.986	.993	.991	.989	.988	.956
Week 5	.999	.960	.993	.998	.964	.980	.995	.973
Week 6	.634**	.988	.904	.996	.961	.992	.878	.907
Week 7	.989	.992	.991	.997	.977	.996	.998	.982
Week 14	.999	.945	.998	.999	.995	.995	.999	.998
Week 21	.995	.972	.991	.979	.975	.984	.997	.977
Week 35	.976	.971	.991	.999	.987	.992	.993	.941

Table 12: Results of correlation analysis showing the r values and significance levels of each gene. Correlation analysis r values for all genes are given here. The Ct values of animals of same age and same gene correlate significantly at 0.01 level except for GAPDH, PACE4 and PC2 at week 3, for which the correlation is significant at 0.05 level (*), and GAPDH at week 6, where the correlation is marginally significant (**).

Expression of SPCs During Postnatal Development of the Visual Cortex: Widely Expressed Members

The $\Delta\Delta\text{Ct}$ value for each age of wt mice was calculated by subtracting the ΔCt of the target age from ΔCt of week 35. Bonferroni-adjusted post-hoc analyses showed that the expression of furin, PACE4, PC5, and PC7 showed significant changes during visual cortex development (Figure 6). Expression of furin was significantly higher in week 1 compared to weeks 3 and 5, and the expression of PACE4 was significantly higher in week 1 compared to weeks 2, 5 and 14. Expression of PC5 was significantly higher in weeks 1 and 3 compared to weeks 5 and 14. Finally, PC7 expression was significantly higher in week 1 compared to weeks 4, 5 and 6. Expression of PC7 was very low in week 5.

Expression of Tissue-Specific SPCs

Bonferroni-adjusted post-hoc analyses for the expression of tissue-specific SPCs showed that the expression of both PC1 and PCSK9 were subjected to significant changes during development (Figure 7). Expression of PC1 was significantly higher in week 7 than in weeks 1, 3, 5 and 21. There was higher expression of PCSK9 in week 1 than in weeks 4, 5, 6, 7 and 21. There was no significant change in the expression of PC2 during visual cortex development.

Expression of SPCs During Retinal Degeneration: Widely Expressed Members

The $\Delta\Delta\text{Ct}$ value for each age was calculated by subtracting the ΔCt of wt from the ΔCt of rd. Bonferroni-adjusted post-hoc analyses showed that the expression of furin, PACE4, PC5 and PC7 was significantly different in rd mice (Figure 8). Expression of furin was significantly lower in week 1 in rd mice compared to all other ages; the expression of PACE4 was also lower in week 1 compared to all other ages except for week 5. The statistical analysis also showed that the expression of PC5 and PC7 was significantly lower in week 1 compared to all other ages.

Expression of Tissue-Specific SPCs

Bonferroni-adjusted post-hoc analyses for the expression of tissue specific SPCs in rd mice showed that the expression of PC1 and PCSK9 was significantly different in rd mice (Figure 9). Expression of PC1 was significantly higher in week 7 than in weeks 1, 3, 5 and 21. There was higher expression of PCSK9 in week 1 than in weeks 4, 5, 6, 7 and 21. There was no significant difference in the expression of PC2 in age during retinal degeneration.

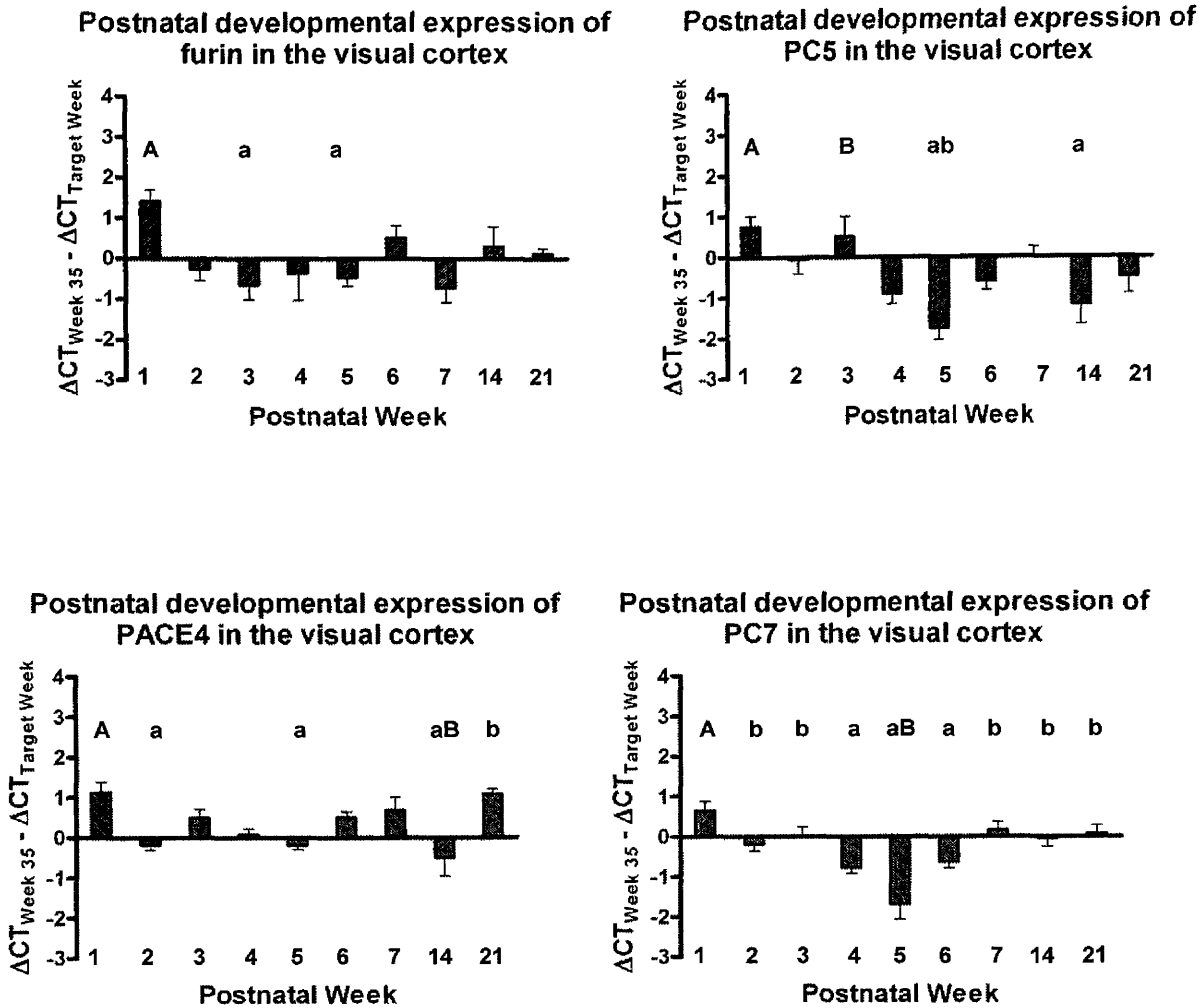


Figure 6. Postnatal developmental expression of widely expressed SPCs in the visual cortex of mice. $\Delta\Delta Ct$ was calculated for each age and each gene. The $\Delta\Delta Ct$ was plotted and values were analyzed for statistical significance. Significant differences between ages are indicated by letters. For example, A and a above the bars indicate that those two time points have a significant difference in the expression of that particular gene. Bonferroni-adjusted post-hoc analyses show that the expression of furin was significantly higher in week 1 compared to weeks 3 and 5 and the expression of PACE4 was significantly higher in week 1 compared to week 2, 5 and 14. Expression of PC5 was significantly higher in weeks 1 and 3 compared to weeks 5 and 14. Finally, PC7 expression was significantly high in week 1 compared to weeks 4, 5 and 6. Expression of PC7 was very low in week 5.

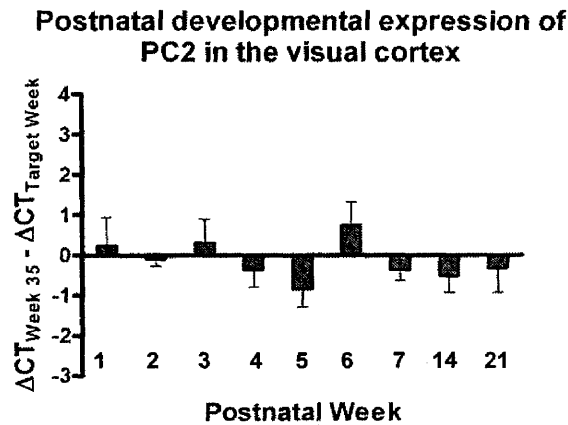
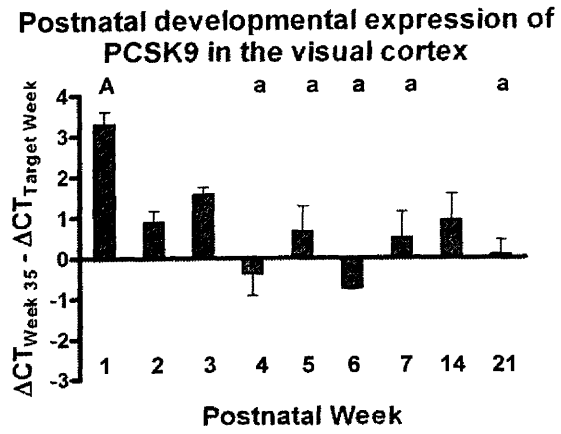
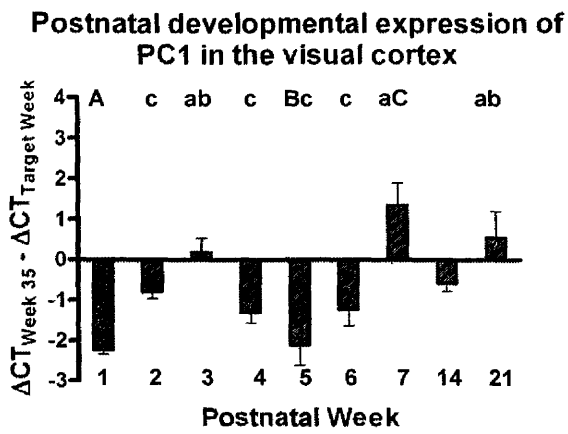


Figure 7: Postnatal developmental expression of tissue-specific SPCs in the visual cortex of mice. $\Delta\Delta\text{Ct}$ was calculated for each age and each gene. The $\Delta\Delta\text{Ct}$ was plotted and values were analyzed for statistical significance. Significant differences between ages are indicated by letters. For example, A and a above the bars indicate that those two time points have a significant difference in the expression of that particular gene. Bonferroni-adjusted post-hoc analyses show that the expression of PC1 was significantly higher in week 7 than in weeks 1, 3, 5 and 21. There was higher expression of PCSK9 in week 1 than in weeks 4, 5, 6, 7 and 21. There was no significant difference in the expression of PC2 during the visual cortex development.

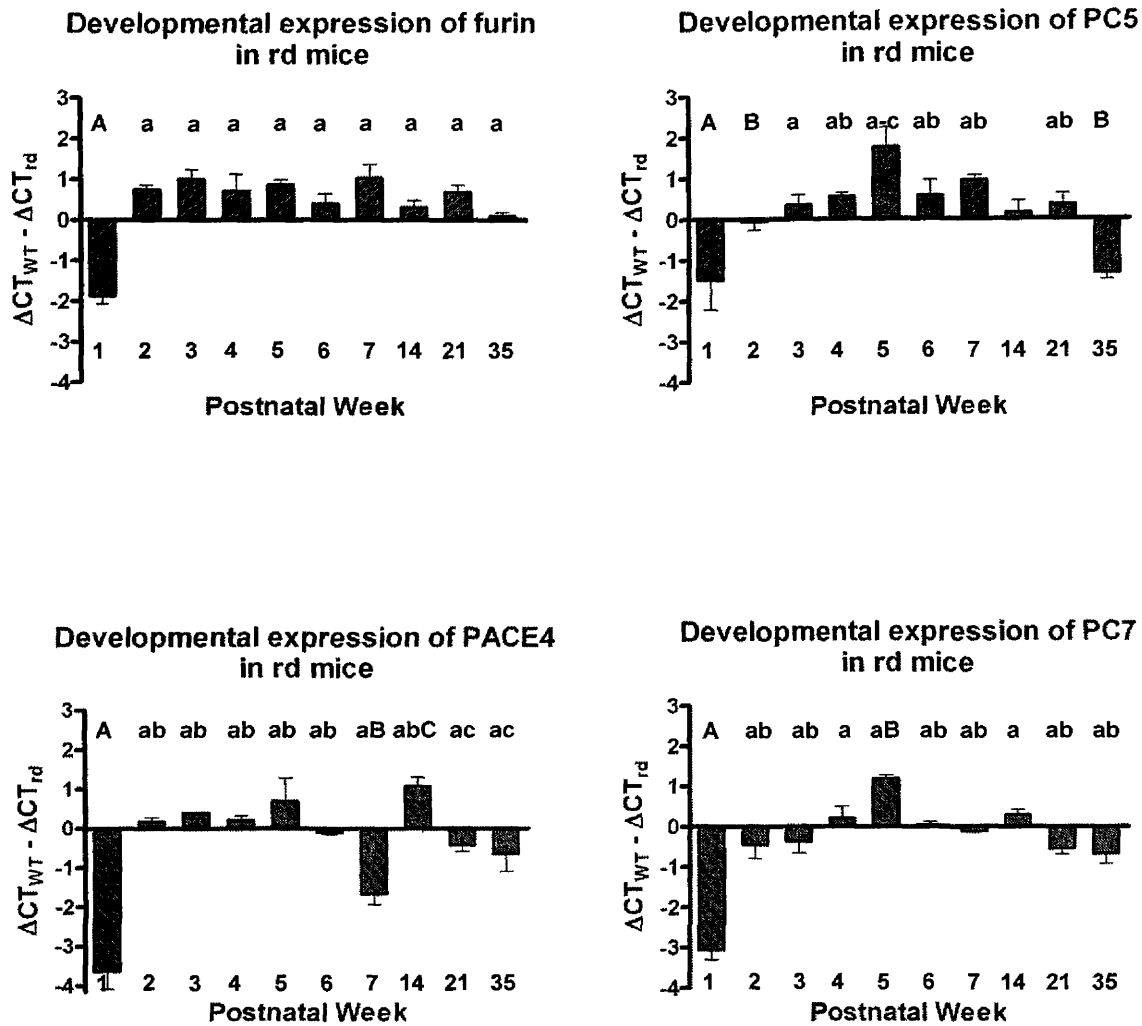


Figure 8: Postnatal developmental expression of widely expressed SPCs in the visual cortex of mice during retinal degeneration. $\Delta\Delta Ct$ was calculated for each age and each gene. The $\Delta\Delta Ct$ was plotted and values were analyzed for statistical significance. Significant differences between ages are indicated by letters. For example, A and a above the bars indicate that those two time points have a significant difference in the expression of that particular gene. Bonferroni-adjusted post-hoc analyses show that the expression of furin was significantly lower in week 1 in rd mice compared to all other ages. The expression of PACE4 was also low in week 1 compared to all other ages except for week 5. The statistical analysis also showed that the expression of PC5 and PC7 were significantly lower in week 1 compared to all other ages.

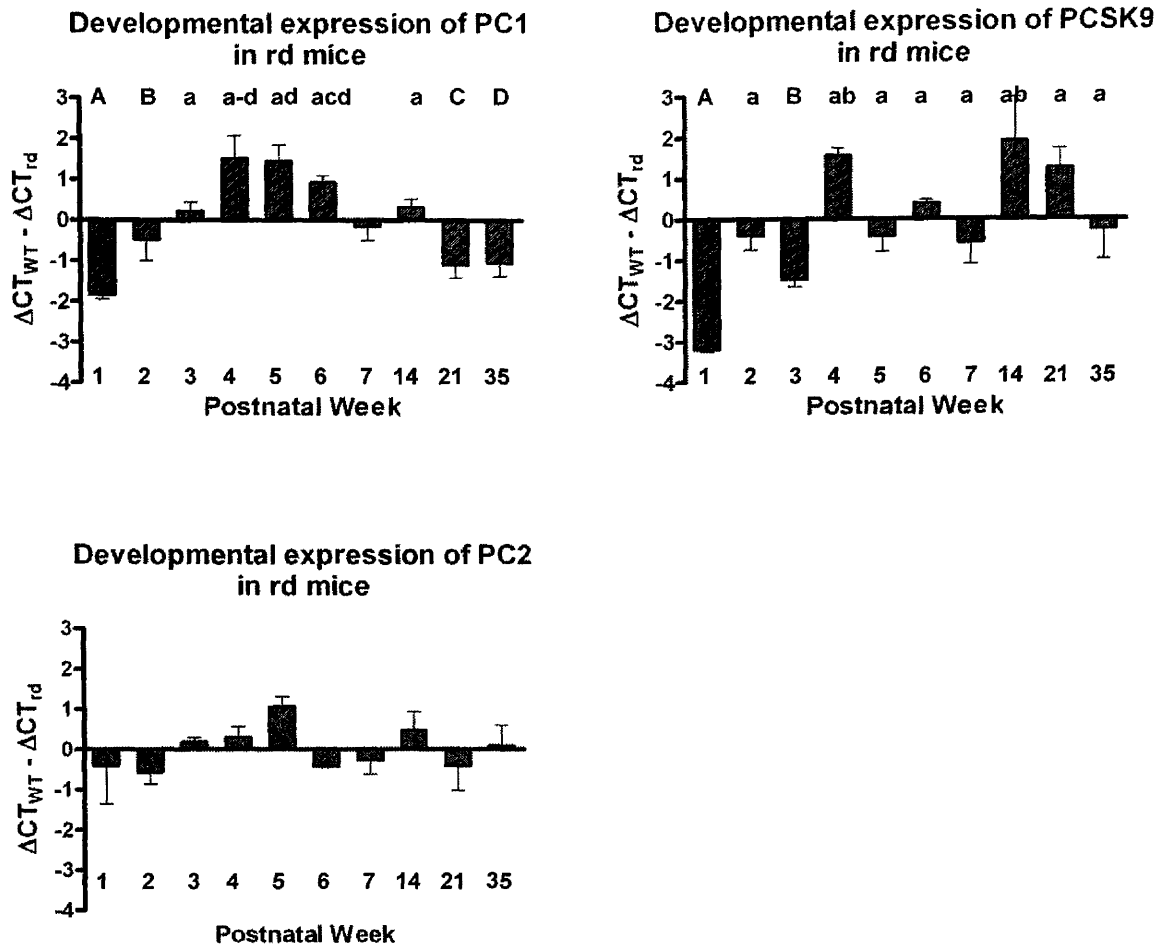


Figure 9: Postnatal developmental expression of tissue-specific SPCs in the visual cortex of mice during retinal degeneration. $\Delta\Delta Ct$ was calculated for each age and each gene. The $\Delta\Delta Ct$ was plotted and values were analyzed for statistical significance. Significant differences between ages are indicated by letters. For example, A and a above the bars indicate that those two time points have a significant difference in the expression of that particular gene. Bonferroni-adjusted post-hoc analyses show that the expression of PC1 was significantly higher in week 7 than in weeks 1, 3, 5 and 21. There was higher expression of PCSK9 in week 1 than in weeks 4, 5, 6, 7 and 21. There was no significant difference in the expression of PC2 in age during retinal degeneration.

Chapter 4: Discussion

SPCs play a very important role in development and homeostasis, and they are also involved in numerous pathologies (Seidah et al. 1999). They play a critical role in the development of visual cortex by processing growth factors like neurotrophins; they also process receptors and neuropeptides and help to maintain cholesterol homeostasis. We studied the expression of SPCs during postnatal developmental of the visual cortex in mice using quantitative real-time PCR. SPCs are also involved in neurodegenerative disease; therefore, the expression of SPCs during retinal degeneration was also studied. Knowing the expression pattern of SPCs during postnatal development of the visual cortex and neurodegenerative disease can provide insight into the overall role of SPCs in brain development and pathology.

Standard and Efficiency Curve Analyses

Standard curve analysis is used to calculate the efficiency of real time PCR. In relative quantification methods, it is assumed that the percentage amplification efficiency (PAE) of the PCR reaction is 100%. However, if the efficiency of the PCR reactions of a particular gene for wt is 100% and rd is 90%, then the comparison made between wt and rd may not be reliable. Thus, it is very important to show that there are no significant differences in amplification efficiencies of wt and rd for all genes. Also, the standard curve of serially diluted samples should give a straight line with a slope of -1. So, all the standard curve lines should have a slope that is not significantly different from -1.

The regression analysis showed that the slope of wt mice was not significantly different from the slope of rd mice at both time points (Table 10 and 11). The regression analysis also showed that the lines were not significantly different from -1 for the wt and rd mice of both time points for all genes, with the exceptions of PC1 at the early time point and furin at the late time point. Although the slopes of PC1 and furin standard curves were significantly different from -1, a correction factor was not used for subsequent analysis. This was because the statistics may not be reliable due to the small sample size. Each standard curve had only five points and the standard curve was done only for four samples. Using small numbers of samples might result in a high standard error. Also, checking the standard curve efficiency of two time points may not reflect the efficiency of other ages. Ideally, one would do the standard curve for each sample at each time point and genotype. Though this would be time consuming and costly, the results would make the data more legitimate. In our study, since all other genes gave the expected result, we did not use the correction factor in the subsequent analysis.

Correlation Analysis

The correlation analysis result showed that the Ct values were highly correlated at the 0.01 level for animals of the same age, same genotype and same gene, except for GAPDH, PACE4 and PC2 of week 3, for which the correlation was significant at 0.05 level, and GAPDH at week 6, which was marginally significant (Table 12). Thus, the Ct values that we obtained are valid for the statistical analysis.

Expression Pattern of SPCs During Normal Development

Expression profiles of both widely expressed and tissue-specific SPCs were obtained. It had been shown that furin, PACE4, PC1, PC2, PC5 and PC7 were expressed in neurons, whereas only furin, PACE4 and PC7 were expressed in glial cells (Bergeron et al, 2000). An earlier study done on the adult rat central nervous system (CNS) using *in situ* hybridization showed that the expression of PC2 was high in cerebral cortex followed by furin and PC1 (Schafer et al., 1993). In another study, using immunohistochemistry on tissue from adult rat CNS, it was shown that PC5 is moderately expressed in cerebral cortex (Villeneuve et al., 1999). Our study, using a more efficient and accurate quantitative real time PCR technique, was consistent with these previous studies showing that the expression of PC2 (mean Ct=24.7) was high in visual cortex of adult mice (week 35) followed by PC1 (mean Ct =29.9), furin (mean Ct =30.4), PACE4 (mean Ct =30.6), PC7 (mean Ct =31.3), and PC5 (mean Ct =31.4). PCSK9 (mean Ct =34.9) was expressed at very low levels compared to other SPCs. As discussed earlier, low Ct values indicate high levels of expression. The developmental expression pattern of widely expressed SPCs were different from tissue specific SPCs. The levels of the widely expressed SPCs were elevated in week 1. Furin and PACE4 expression was reduced in week 2 and essentially stabilized at adult levels. The expression of PC5 and PC7 also decreased to adult levels in week 2, but then became significantly reduced by week 5.

The alterations of SPC expression could have implications for postnatal visual cortex development. The first week of postnatal development, where higher levels of widely expressed SPCs was observed, is the time when refinement of the retinotopic map

takes place. The term retinotopic map refers to the existence of a non-random relationship between the positions of neurons in the visual cortex of the brain and the retina. The wiring of the connections between the neurons in retinotopic map takes place during the first week of life without any visual stimuli (before eye opening) (Cang et al., 2005). Later, when the retina receives visual stimuli, the refinement of the neural connections occurs. It has been shown that the neurotrophin, NT-3, is involved in retinotopic map formation. NT-3 is a substrate for furin, PACE4 and PC5 (Seidah et al., 1996). Increased levels of these widely expressed SPCs during the first postnatal week might promote processing of NT-3, making mNT-3 constitutively available for the neurons, which in turn stimulates retinotopic map formation. High expression of furin, PACE4, PC5 and PC7 during the first week of development could also help in processing of pro-NGF and pro-BDNF (Seidah et al., 1996). Expression of BDNF has been shown to increase during postnatal week 1 to 4 (Luckman et al., 2008). The decrease in expression of furin, PACE4 and PC5 seen during weeks 2 to week 4 might cause an increase in the production of pro-NGF and pro-BDNF. These pro-forms of neurotrophins can cause apoptosis by binding to p75NTR, because pro-NGF and pro-BDNF have high affinity for p75NTR in the presence of a co-receptor called sortilin (Nykjaer et al., 2004). Mature forms of NGF and BDNF cause the neurons receiving them to survive, whereas, pro-NGF and pro-BDNF can induce apoptosis (Pedraza et al., 2005).

Among the tissue-specific SPCs, the expression of PC2 remains unchanged during postnatal development of the visual cortex. PC2 is highly expressed in the visual cortex and it might play an important role in processing critical neuropeptides. The pro-forms of some neurotrophins may be processed in the regulated secreted pathway by

PC1, which occurs in secretory vesicles in response to external stimuli. PCSK9 expression is high in week 1 and then it decreases in consecutive weeks. PCSK9 may play a very important role in regulating the uptake of cholesterol by degrading LDLR (Qian et al., 2007), and cholesterol is needed for synaptogenesis (Hanaka et al., 2000). Decreased PCSK9 in later time points may promote increased cholesterol uptake. Interestingly, upregulation of PCSK9 has been suggested to be a critical part of CNS development (Poirier et al., 2006), a result seemingly inconsistent with the role of cholesterol in synaptogenesis and retinotopic map formation. We should also point out that, since PCSK9 is secreted, it may not locally impact LDLR degradation and cholesterol uptake.

Expression Pattern of SPCs During Retinal Degeneration

The expression pattern of the widely expressed SPCs in rd mice was markedly different from that of wt mice. The widely expressed SPCs were present at low levels in week 1 and the amount of mRNA increased over the next few weeks. Processing of pro-neurotrophins, particularly pro-NT-3, is very important in the first week of development. Lack of mature NT-3 may disrupt retinotopic map formation, which is very important for ocular dominance plasticity (the effect of experience in development of the visual cortex). If the retinotopic map is not established in the first week of postnatal development, ocular dominance plasticity will not occur properly, even in the presence of visual stimuli. The expression of furin and PACE4 reaches the adult level from week 2 onwards. Rd mice lose vision gradually over the few postnatal months due to the death of rods and cones in retina. As vision is being lost, neurons in the visual cortex tend to establish new connections in an attempt to remain viable, because in the decrease or

absence of visual stimuli, these neurons undergo apoptosis. So, to remain viable, neurons forms new connections (synapses) with neighboring neurons, which likely requires mature forms of neurotrophins. Furin and PACE4 may help in processing pro-neurotrophins, which would aid in the formation of new synaptic connections. PC5 and PC7 can also activate pro-neurotrophins. Higher levels of expression of PC5 and PC7 seen at week 5 may also play a vital role in processing pro form of neurotrophins and establish new synaptic connections.

The expression of PC2 did not change during retinal degeneration. The expression of PC1 is low at early time points and increases during weeks 4, 5 and 6. PC1 might help to process the pro neurotrophins, notably pro-BDNF, in the regulated secretory pathway. The expression of PCSK9 is low in the first three weeks of retinal degeneration and it reached adult level at week 4. PCSK9 may play an important role in cholesterol uptake which is needed for synapses formation. However, as discussed earlier, PCSK9 may not act locally in visual cortex.

We have studied the expression of SPCs in the visual cortex only at the mRNA level. High levels of mRNA expression of a particular gene don't necessarily mean that there is a correspondingly high level of that protein. There are many steps between mRNA and a functionally active protein. The mRNA may be regulated at the level of stability, or its access to the translational machinery could be controlled. Further, even if SPCs are translated, post translational modifications and trafficking must occur before they become functionally active endoproteases. Future studies should focus on the expression of SPCs at the protein level during development of the visual cortex.

Our study provides a foundation for understanding the expression of SPCs at the mRNA level during development of the visual cortex, and how this expression changes during retinal degeneration. We have observed different expression patterns for widely expressed and tissue-specific members of the SPC family, and different patterns in wt and rd mice. This study will provide context for future research to answer additional questions. What regulates these SPC gene expressions during development? What is happening to the expression of SPCs at protein level? Are there other targets for SPCs, beside neurotrophins and neuropeptides, which play an important role in brain development? SPCs play a vital role in neurodegenerative diseases. In our study the expression of SPCs was significantly altered during retinal degeneration. Understanding the role of SPCs during brain development and neurodegenerative diseases will ultimately lead to the finding the therapeutic treatment for such diseases.

References

1. Akamatsu, T., Shigeo Daikoku, Hideaki Nagamune, Shigeru Yoshida, Kenji Mori, Akihiko Tsuji, and Yoshiko Matsuda. 1997. Developmental expression of a novel kexin family protease, PACE4E, in the rat olfactory system. *Histochem Cell Biol.* Vol, 108:95–103.
2. Barres, B.A., and Stephen J. Smith. 2001. Neurobiology cholesterol-making or breaking the synapse. *Science.* Vol, 294: 1296-1297.
3. Bengoetxea, H., Enrike G.Argandon, and Jose V.Lafuente. 2008. Effects of visual experience on vascular endothelial growth factor expression during the postnatal development of the rat visual cortex. *Cerebral Cortex.* Vol, 18:1630-1639.
4. Berardi, N., and Lamberto Maffei. 1999. From visual experience to visual function: Roles of neurotrophins. *Journal of neurobiology.* Vol, 41:119-126.
5. Berardi, N., Tommaso Pizzorusso¹, Gian Michele Ratto, and Lamberto Maffei. 2003. Molecular basis of plasticity in the visual cortex. *Trends in Neurosciences.* Vol, 26(7): 369-378.
6. Caleo, M., and Lamberto Maffei. 2002. Neurotrophins and plasticity in the visual cortex. *The Neuroscientist.* Vol, 8: 52.
7. Cang, J., Rene C. Renteria, Megumi Kaneko, Xiaorong Liu, David R. Copenhagen, and Michael P. Stryker. 2005. Development of precise maps in visual cortex requires patterned spontaneous activity in the retina. *Neuron.* Vol, 48(5): 797–809.

8. Chao, M., Patrizia Casaccia Bonnefil, Bruce Carter, Alexandra Chittka, Haeyoung Kong, and Sung Ok Yoon. 1998. Neurotrophin receptors: mediators of life and death. *Brain Research Reviews*. Vol, 26: 295–301.
9. Fagiolini, M., Tommaso Pizzorusso, Nicoletta Berardi, Luciano Domenici, and Lamberto Maffei. 1994. Functional postnatal development of the rat primary visual cortex and the role of visual experience: Dark rearing and monocular deprivation. *Vision Res*. Vol, 34 (6): 709-720.
10. Farhadi, H.F., S. Javad Mowla, Kevin Petrecca, Stephen J. Morris, Nabil G. Seidah, and Richard A. Murphy. 2000. Neurotrophin-3 sorts to the constitutive secretory pathway of hippocampal neurons and is diverted to the regulated secretory pathway by coexpression with brain-derived neurotrophic factor. *The Journal of Neuroscience*. Vol, 20(11):4059–4068.
11. Hanaka, S., Toshiaki Abe, Hiroshige Itakura, and Akiyo Matsumoto. 2000. Gene expression related to cholesterol metabolism in mouse brain during development. *Brain & Development*. Vol, 22: 321-326.
12. Klein, D. 2002. Quantification using real-time PCR technology: applications and limitations. *Trends in Molecular Medicine*. Vol, 8: 257-260.
13. Morino, W. P., Gunter Rager, Peter Sonderegger, and Detlev Grabs. 2003. Expression of neuroserpin in the visual cortex of the mouse during the developmental critical period. *European Journal of Neuroscience*. Vol, 17: 1853-1860.

14. Nakamura, K., Namekata K., Harada C., and Harada T. 2007. Intracellular sortilin expression pattern regulates pro-NGF induced naturally occurring cell death during development. *Cell Death and Differentiation*. Vol, 14: 1552–1554.
15. Nykjaer, A., Ramee Lee, Kenneth Teng, Pernille Jansen, Peder Madsen, Morten S. Nielsen, Christian Jacobsen, Marco Kliemanne, Elisabeth Schwarz, Thomas E. Willnow, Barbara L. Hempstead, and Claus M. Petersen. 2004. Sortilin is essential for pro-NGF induced neuronal cell death. *Nature*. Vol, 427: 843-847.
16. Pedraza, C. E., Petar Podlesniy, Noem Vida, Juan Carlos Arevalo, Ramee Lee, Barbara Hempstead, Isidre Ferrer, Montse Iglesias, and Carme Espinet. 2005. Pro-NGF isolated from the human brain affected by alzheimer's disease induces neuronal apoptosis mediated by p75NTR. *American Journal of Pathology*. Vol, 166: 533-543.
17. Pfaffl, M.W. 2001. A new mathematical model for relative quantification in real-time RT-PCR. *Nucleic Acids Research*. Vol, 29 (9):2003-2007.
18. Pizzorusso, T., Michela Fagiolini, Laura Gianfranceschi, Vittorio Porciatti, and Lamberto Maffei. 2000. Role of neurotrophins in the development and plasticity of the visual system: experiments on dark rearing. *International Journal of Psychophysiology*. Vol, 35: 189-196.
19. Poirier, S., Annik Prat, Edwige Marcinkiewicz, Joanne Paquin, Babykumari P. Chitramuthu, David Baranowski, Benoit Cadieux, Hugh P. J. Bennettand, and Nabil G. Seidah. 2006. Implication of the proprotein convertase NARC-1/PCSK9 in the development of the nervous system. *Journal of Neurochemistry*. Vol, 98: 838–850.

20. Qian, W.Y., Robert J. Schmidt, Youyan Zhang, Shaoyou Chu, Aimin Lin, He Wang, Xiliang Wang, Thomas P. Beyer, William R. Bensch, Weiming Li, Mariam E. Ehsani, Deshun Lu, Robert J. Konrad, Patrick I. Eacho, David E. Moller, Sotirios K. Karathanasis, and Guoqing Cao. 2007. Secreted PCSK9 downregulates low density lipoprotein receptor through receptor-mediated endocytosis. *Journal of Lipid Research*. Vol, 48:1488-1498.
21. Riddle, D.R. 1995. NT-4-mediated rescue of lateral geniculate neurons from effects of monocular deprivation. *Nature*. Vol, 378: 189–191.
22. Schafer, K.H., Robert Day, William E. Cullinan, Michel Chretien, Nabil G. Seidah, and Stanley J. Watson. 1993. Gene expression of prohormone and proprotein convertases in the rat CNS: A comparative *in situ* hybridization analysis. *The Journal of Neuroscience*. Vol, 73(3): 1258-1279
23. Seidah N.G., Chrgtien M, and R Day. 1994. The family of subtilisin/kexin like pro-protein and pro-hormone convertases: Divergent or shared functions. *Biochimie*. Vol, 76: 197-209.
24. Seidah N.G., Gaetan Mayer, Ahmed Zaid, Estelle Rousselet, Nasha Nassoury, Steve Poirier, Rachid Essalmani, and Annik Prat. 2008. The activation and physiological functions of the proprotein convertases. *The International Journal of Biochemistry & Cell Biology*. Vol, 40: 1111–1125.
25. Seidah N.G., Suzanne Benjannet, Sangeeta Pareek, Diane Savaria, Jose. E Hamelin, Brigitte Goulet, Jacynthe Laliberte, Claude Lazure, Michel Chre, Tien and Richard A. Murphy. 1996. Cellular processing of the nerve growth factor

- precursor by the mammalian pro-protein convertases. *Biochem. J.* Vol, 314: 951-960.
26. Seidah N.G., Suzanne Benjannet, Sangeeta Pareek, Michel Chrôtien, and Richard A. Murphy. 1996. Cellular processing of the neurotrophin precursors of NT3 and BDNF by the mammalian proprotein convertases. *FEBS Letters.* Vol, 379: 247-250.
27. Temburni M., and Michele H. Jacob. 2001. New functions for glia in the brain. *PNAS.* Vol, 98: 3631–3632.
28. Tropea D., Audra Van Wart, and Mriganka Sur. 2009. Molecular mechanisms of experience-dependent plasticity in visual cortex. *Phil. Trans. R. Soc. B.* Vol, 364: 341–355.
29. Tsuji A., Chiemi Hine, Kenji Mori, Yasuhiro Tamai, Kazuya Higashine, Hideaki Nagamune, and Yoshiko Matsuda. 1994. A novel member, PC7, of the mammalian kexin-like protease family: Homology to PACE4, its brain specific expression and identification of isoforms. *Biochemical and Biophysics Research Communication.* Vol, 202:1452-1459.
30. Valasek M.A., and Joyce J. Repa. 2005. The power of real-time PCR. *Adv Physiol Educ.* Vol, 29: 151–159.
31. Villeneuve, P., N. G. Seidah, and A. Beaudet. 1999. Immunohistochemical distribution of the prohormone convertase PC5-A in rat brain. *Neuroscience.* Vol, 92: 641–654.

32. Wahle, P. 2003. Differential effects of cortical neurotrophic factors on development of lateral geniculate nucleus and superior colliculus neurons: anterograde and retrograde actions. *Development*. Vol, 130: 611–622.
33. Yuan S.J., Ann Reed, Feng Chen, and C Neal Stewart. 2006. Statistical analysis of real-time PCR data. *BMC Bioinformatics*. Vol, 7:85

Appendices

Appendix 1: Data for Standard Curve Analysis for Wt and Rd at the Early Time Point

Animal	Gene	cDNA	LogBase		plustype	interaction	minustype	interaction2
			2cDNA_mean	Ct_mean				
Rd	Furin	0.0001	-13.29	42.625	0	0	1	-13.29
Rd	Furin	0.001	-9.97	38.465	0	0	1	-9.97
Rd	Furin	0.01	-6.64	36.935	0	0	1	-6.64
Rd	Furin	0.1	-3.32	33.275	0	0	1	-3.32
Rd	Furin	1	0	30.02	0	0	1	0
Wt	Furin	0.0001	-13.29	41.6	1	-13.29	0	0
Wt	Furin	0.001	-9.97	37.05	1	-9.97	0	0
Wt	Furin	0.01	-6.64	35.785	1	-6.64	0	0
Wt	Furin	0.1	-3.32	31.32	1	-3.32	0	0
Wt	Furin	1	0	28.245	1	0	0	0
Rd	GAPDH	0.0001	-13.29	34.4	0	0	1	-13.29
Rd	GAPDH	0.001	-9.97	31.66	0	0	1	-9.97
Rd	GAPDH	0.01	-6.64	27.83	0	0	1	-6.64
Rd	GAPDH	0.1	-3.32	23.825	0	0	1	-3.32
Rd	GAPDH	1	0	20.055	0	0	1	0
Wt	GAPDH	0.0001	-13.29	35.48	1	-13.29	0	0
Wt	GAPDH	0.001	-9.97	31.195	1	-9.97	0	0
Wt	GAPDH	0.01	-6.64	27.57	1	-6.64	0	0
Wt	GAPDH	0.1	-3.32	24.94	1	-3.32	0	0
Wt	GAPDH	1	0	20.1	1	0	0	0
Rd	PACE4	0.008	-6.97	36.145	0	0	1	-9.97
Rd	PACE4	0.04	-4.64	33.51	0	0	1	-6.64
Rd	PACE4	0.2	-2.32	30.91	0	0	1	-3.32
Rd	PACE4	1	0	28.2	0	0	1	0
Wt	PACE4	0.008	-6.97	35.125	1	-6.97	0	0
Wt	PACE4	0.04	-4.64	33.745	1	-4.64	0	0
Wt	PACE4	0.2	-2.32	31.28	1	-2.32	0	0
Wt	PACE4	1	0	27.58	1	0	0	0
Rd	PC1	0.0001	-13.29	39.455	0	0	1	-13.29
Rd	PC1	0.001	-9.97	36.88	0	0	1	-9.97
Rd	PC1	0.01	-6.64	33.66	0	0	1	-6.64
Rd	PC1	0.1	-3.32	30.82	0	0	1	-3.32
Rd	PC1	1	0	27.42	0	0	1	0
Wt	PC1	0.0001	-13.29	39.335	1	-13.29	0	0
Wt	PC1	0.001	-9.97	36.08	1	-9.97	0	0
Wt	PC1	0.01	-6.64	32.655	1	-6.64	0	0
Wt	PC1	0.1	-3.32	30.155	1	-3.32	0	0
Wt	PC1	1	0	26.865	1	0	0	0
Rd	PC2	0.0001	-13.29	38.085	0	0	1	-13.29
Rd	PC2	0.001	-9.97	36.32	0	0	1	-9.97
Rd	PC2	0.01	-6.64	33.765	0	0	1	-6.64
Rd	PC2	0.1	-3.32	31.535	0	0	1	-3.32

Rd	PC2	1	0	23.92	0	0	1	0
Wt	PC2	0.0001	-13.29	37.335	1	-13.29	0	0
Wt	PC2	0.001	-9.97	35.4	1	-9.97	0	0
Wt	PC2	0.01	-6.64	33.485	1	-6.64	0	0
Wt	PC2	0.1	-3.32	30.65	1	-3.32	0	0
Wt	PC2	1	0	20.57	1	0	0	0
Rd	PC5	0.001	-9.97	38.6	0	0	1	-9.97
Rd	PC5	0.01	-6.64	35.15	0	0	1	-6.64
Rd	PC5	0.1	-3.32	32.94	0	0	1	-3.32
Rd	PC5	1	0	29.165	0	0	1	0
Wt	PC5	0.001	-9.97	36.71	1	-9.97	0	0
Wt	PC5	0.01	-6.64	34.565	1	-6.64	0	0
Wt	PC5	0.1	-3.32	31.32	1	-3.32	0	0
Wt	PC5	1	0	26.21	1	0	0	0
Rd	PC7	0.001	-9.97	40.73	0	0	1	-9.97
Rd	PC7	0.01	-6.64	38.75	0	0	1	-6.64
Rd	PC7	0.1	-3.32	33.68	0	0	1	-3.32
Rd	PC7	1	0	28.095	0	0	1	0
Wt	PC7	0.001	-9.97	39.245	1	-9.97	0	0
Wt	PC7	0.01	-6.64	35.945	1	-6.64	0	0
Wt	PC7	0.1	-3.32	33.085	1	-3.32	0	0
Wt	PC7	1	0	24.775	1	0	0	0

Appendix 2: Data for Standard Curve Analysis for Wt and Rd at the Later Time Point

Animal	Gene	cDNA	LogBase2		plustype	interaction	minustype	interaction2
			cDNA_mean	Ct_mean				
Rd	Furin	0.0001	-13.29	37.29	0	0	1	-13.29
Rd	Furin	0.001	-9.97	34.98	0	0	1	-9.97
Rd	Furin	0.01	-6.64	32.64	0	0	1	-6.64
Rd	Furin	0.1	-3.32	29.87	0	0	1	-3.32
Rd	Furin	1	0	26.58	0	0	1	0
Wt	Furin	0.0001	-13.29	38.54	1	-13.29	0	0
Wt	Furin	0.001	-9.97	36.24	1	-9.97	0	0
Wt	Furin	0.01	-6.64	33.95	1	-6.64	0	0
Wt	Furin	0.1	-3.32	30.56	1	-3.32	0	0
Wt	Furin	1	0	27.36	1	0	0	0
Rd	GAPDH	0.0001	-13.29	35.165	0	0	1	-13.29
Rd	GAPDH	0.001	-9.97	31.465	0	0	1	-9.97
Rd	GAPDH	0.01	-6.64	29.22	0	0	1	-6.64
Rd	GAPDH	0.1	-3.32	24.575	0	0	1	-3.32
Rd	GAPDH	1	0	21.145	0	0	1	0
Wt	GAPDH	0.0001	-13.29	32.125	1	-13.29	0	0
Wt	GAPDH	0.001	-9.97	28.66	1	-9.97	0	0
Wt	GAPDH	0.01	-6.64	25.26	1	-6.64	0	0
Wt	GAPDH	0.1	-3.32	22.82	1	-3.32	0	0
Wt	GAPDH	1	0	18.61	1	0	0	0
Rd	PACE4	0.0016	-9.29	38.64	0	0	1	-13.29
Rd	PACE4	0.008	-6.97	37.405	0	0	1	-9.97
Rd	PACE4	0.04	-4.64	35.92	0	0	1	-6.64
Rd	PACE4	0.2	-2.32	33.485	0	0	1	-3.32
Rd	PACE4	1	0	26.945	0	0	1	0
Wt	PACE4	0.0016	-9.29	36.875	1	-9.29	0	0
Wt	PACE4	0.008	-6.97	35.455	1	-6.97	0	0
Wt	PACE4	0.04	-4.64	32.835	1	-4.64	0	0
Wt	PACE4	0.2	-2.32	31.46	1	-2.32	0	0
Wt	PACE4	1	0	25.455	1	0	0	0
Rd	PC1	0.001	-9.97	38.18	0	0	1	-9.97
Rd	PC1	0.01	-6.64	36.55	0	0	1	-6.64
Rd	PC1	0.1	-3.32	34.62	0	0	1	-3.32
Rd	PC1	1	0	28.315	0	0	1	0
Wt	PC1	0.0001	-13.29	37.17	1	-13.29	0	0
Wt	PC1	0.001	-9.97	35.915	1	-9.97	0	0
Wt	PC1	0.01	-6.64	33.835	1	-6.64	0	0
Wt	PC1	0.1	-3.32	30.13	1	-3.32	0	0
Wt	PC1	1	0	24.965	1	0	0	0
Rd	PC2	0.0001	-13.29	34.77	0	0	1	-13.29
Rd	PC2	0.001	-9.97	31.26	0	0	1	-9.97
Rd	PC2	0.01	-6.64	29.875	0	0	1	-6.64

Rd	PC2	0.1	-3.32	27.455	0	0	1	-3.32
Rd	PC2	1	0	22.21	0	0	1	0
Wt	PC2	0.0001	-13.29	31.37	1	-13.29	0	0
Wt	PC2	0.001	-9.97	29.68	1	-9.97	0	0
Wt	PC2	0.01	-6.64	28.47	1	-6.64	0	0
Wt	PC2	0.1	-3.32	25.115	1	-3.32	0	0
Wt	PC2	1	0	19.44	1	0	0	0
Rd	PC5	0.008	-6.97	36.21	0	0	1	-9.97
Rd	PC5	0.04	-4.64	34.87	0	0	1	-6.64
Rd	PC5	0.2	-2.32	32.815	0	0	1	-3.32
Rd	PC5	1	0	29.77	0	0	1	0
Wt	PC5	0.0016	-9.29	38.375	1	-9.29	0	0
Wt	PC5	0.008	-6.97	36.275	1	-6.97	0	0
Wt	PC5	0.04	-4.64	32.645	1	-4.64	0	0
Wt	PC5	0.2	-2.32	30.35	1	-2.32	0	0
Wt	PC5	1	0	28.525	1	0	0	0
Rd	PC7	0.0016	-9.29	36.14	0	0	1	-13.29
Rd	PC7	0.008	-6.97	34.5	0	0	1	-9.97
Rd	PC7	0.04	-4.64	32.605	0	0	1	-6.64
Rd	PC7	0.2	-2.32	29.66	0	0	1	-3.32
Rd	PC7	1	0	26.425	0	0	1	0
Wt	PC7	0.0016	-9.29	35.46	1	-9.29	0	0
Wt	PC7	0.008	-6.97	33.465	1	-6.97	0	0
Wt	PC7	0.04	-4.64	30.595	1	-4.64	0	0
Wt	PC7	0.2	-2.32	27.31	1	-2.32	0	0
Wt	PC7	1	0	25.41	1	0	0	0

Appendix 3: Syntax for Regression Analysis

```
SORT CASES BY Gene .  
SPLIT FILE  
  LAYERED BY Gene .
```

```
GRAPH  
/SCATTERPLOT(BIVAR)=LogBase2cDNA_mean WITH Ct_mean BY Treatment  
/MISSING=LISTWISE .
```

```
REGRESSION  
/MISSING LISTWISE  
/STATISTICS COEFF OUTS CI R ANOVA  
/CRITERIA=PIN(.05) POUT(.10)  
/NOORIGIN  
/DEPENDENT Ct_mean  
/METHOD=ENTER LogBase2cDNA_mean plustype interaction .
```

```
REGRESSION  
/MISSING LISTWISE  
/STATISTICS COEFF OUTS CI R ANOVA  
/CRITERIA=PIN(.05) POUT(.10)  
/NOORIGIN  
/DEPENDENT Ct_mean  
/METHOD=ENTER LogBase2cDNA_mean minustype interaction2 .
```

Appendix 4: Data for actual runs. High and low Ct values for all the genes

Geno-type	Age	GAPDH hi	GAPDH low	Furin hi	Furin low	PACE4 hi	PACE4 low	PC1 hi	PC1 low	PC2 hi	PC2 low	PC5 hi	PC5 low	PC7 hi	PC7 low	PCSK9 hi
Wt	Week1	22.3	22.25	31.2	31	32	31.7	35.7	35.5	26.8	26.4	34.9	34.5	32.9	32.9	33.2
Wt	Week1	21.05	21.02	28.5	28.5	28.6	28.5	30.3	30	23.8	23.6	29.2	29.1	29.7	29.4	30.3
Wt	Week1	22.42	22.32	29.5	29.7	30.3	29.6	34	33.8	25.1	25	31.6	31.5	31.2	30.9	32.1
Wt	Week1	23.17	23.16	29.69	29.57	30.82	30.7	33.25	33.09	25.96	25.9	32.32	32.03	32.33	31.9	33.32
Rd	Week1	22.67	22.59	31.5	31.3	33.7	33.4	33.8	33.7	23.9	23.8	31.5	31	34.3	33.9	35.4
Rd	Week1	23.64	23.36	33.4	32.9	34.4	33.8	35.8	35	27.8	27.6	33.9	33.6	34.9	34.8	35.9
Rd	Week1	22.8	22.79	31.2	31.1	35.2	34.5	36	36	26.7	26.7	35.2	34.9	35.3	35.2	36.9
Wt	Week2	22.61	22.27	30.8	30.6	31.5	31.4	30.2	30.1	25.5	25.5	31.9	31.2	31.6	31.5	35
Wt	Week2	21.62	21.5	30.2	30.1	30.8	30.5	31.6	31.5	25.6	25.4	31.6	30.9	31.9	31.8	34.5
Wt	Week2	22.73	22.19	31.8	31.8	31.1	30.8	31.2	30.8	24.9	24.2	32.3	32.3	31.7	31.5	34.1
Rd	Week2	21.65	21.32	29.5	29.3	30.2	30	30.8	30.3	24.3	24.3	30.7	30.7	31.4	31.3	34.5
Rd	Week2	22.75	22.68	30.4	30.3	31.1	30.9	30.1	30	25.8	25.5	31.5	31.5	32.7	32.7	35.3
Rd	Week2	21.13	20.99	29.6	29.3	30.6	30.5	30.7	30.6	25	25	30.9	30.6	31.8	31.7	33.7
Rd	Week2	20.61	20.53	29.5	29.13	30.05	29.42	29.87	29.67	24.55	24.47	30.46	30.32	30.72	30.67	33.43
Wt	Week3	23.19	23.08	33.3	32.9	31.4	31.3	31.1	30.5	25.6	25.5	32.3	32	32.3	32.2	34.7
Wt	Week3	22.66	22.03	31.4	31.2	30.8	30	29.6	29.2	24.9	24.9	31.5	31.2	31.9	31.8	34.8
Wt	Week3	22.36	22.36	30.9	30.8	30.7	30.6	31	31	25.4	25	31.5	31.3	31.8	31.6	33.9
Rd	Week3	21.97	21.94	31.1	30.7	29.8	29.7	29.5	29.5	24.7	24.4	30.8	30.4	31.3	31.2	35.8
Rd	Week3	23.16	23.01	30.3	30	30.8	30.8	31.1	31.1	26.1	25.3	32.6	32.3	33.6	33.5	35.6
Rd	Week3	22.27	22.13	30.6	30.4	30.2	29.9	29.5	29.3	24.3	24.1	31	30.4	31.7	31.2	34.6
Wt	Week4	20.49	20.38	30.7	30.4	29.2	29.2	28.2	28.2	24.2	24.1	30.5	30.2	30.2	29.9	34.2
Wt	Week4	22.57	22.54	30.2	30.1	30.7	30.7	33.6	33	25.1	25	33.1	33	33.1	32.9	34.9
Wt	Week4	21.51	21.42	30.2	30.2	30.3	30.3	30.9	30.7	25.2	25.2	32.4	32.4	31.7	31.7	36.2
Rd	Week4	23.85	23.75	31.6	31.1	32.1	32.1	31.8	31.1	26.8	26.6	33.1	33	33.1	32.6	35.6
Rd	Week4	22.54	22.38	30.7	30.6	30.6	30.5	29.8	29.7	24.9	24.5	32.5	32.1	32.3	32.3	35.6
Rd	Week4	23.49	22.85	31.8	31.8	32.1	31.6	31.5	31.4	27.2	26.8	33.8	33.4	33.9	33.9	34.5
Wt	Week5	22.08	22.06	31.7	31.2	31.8	31.4	34.8	34.5	26.5	26.4	34.8	35	34.6	34.3	34.4
Wt	Week5	22.13	22.03	31.1	31	30.8	30.8	30.9	30.5	25.9	25.1	32.6	31.9	32.7	32.4	36.3
Wt	Week5	22.54	22.45	31.1	30.8	30.9	30.8	31.6	31.6	26.2	25.8	33.6	33.1	32.9	32.5	33.9
Rd	Week5	24.46	24.17	32	31.6	34.4	34.3	34.7	34.6	27.2	27.1	34.7	34.4	35.8	34.9	35.7
Rd	Week5	22.52	22.45	30.9	30.9	29.7	29.1	30.1	30	25.4	25.2	31.1	31.1	31.7	31.6	36.8
Rd	Week5	22.19	22.12	30.5	30.5	29.7	29.6	30.2	30.1	24.8	24.5	31.6	31.4	31.5	31.4	35.6
Wt	Week6	23.6	23.55	31.2	31	31.5	31.3	32.3	32.2	25.7	25.4	32.8	32.5	33.5	33.4	36.6
Wt	Week6	23.62	23.54	31.4	31.1	32.3	31.5	32.6	32.5	25.8	25.5	33.6	33.1	33.4	33.1	36.7
Wt	Week6	23.03	23.02	31.9	31.5	31.8	31.1	33.1	32.9	25.5	25.4	34.8	34.3	33.4	33.3	36.8
Rd	Week6	23	22.73	32.6	32.1	31.6	31.3	31.9	31.8	25.8	25.5	33.5	33.3	33.1	33	36.5
Rd	Week6	22.98	22.89	30.9	30.7	30.9	30.7	30.6	30.3	25.5	25.4	32.3	32.1	32	31.9	36.5
Rd	Week6	23.81	22.93	31	31	32.2	31.5	31.8	31.7	26.6	26.6	33.4	33	33.6	32.8	36.7
Rd	Week6	23.63	23.47	30.79	30.75	31.29	30.95	34.39	34.05	26.21	25.92	32.77	32.42	33.41	33.35	36.02
Wt	Week7	20.99	20.95	31.3	30.8	29.6	29.5	28	28	24.7	24.3	30.3	30.3	30.5	30.3	34.6
Wt	Week7	20.98	20.89	29.8	29.7	29.5	29.3	28.1	28	25.1	24.9	31	31	30.2	30.2	34
Wt	Week7	23.72	23.39	32.4	32.1	30.5	30.4	29.4	29.3	25.9	25.8	32.7	32.6	32.4	32.3	34.9
Rd	Week7	23.67	23.39	31.4	31.3	32.9	32.1	30.5	30.4	26.8	26.7	32.7	32.6	33	32.7	36.5
Rd	Week7	23.33	23.13	30.9	30.6	30.9	30.4	30.1	29.6	26.2	26	31.7	31.1	31.4	31.2	35.4
Rd	Week7	23.29	23.14	31.6	31.4	33.3	32.8	34.6	34	26.1	26.5	35.6	35.2	34.6	34.6	36.7
Rd	Week7	23.53	22.79	32.08	31.81	31.65	30.81	30.04	29.89	24.19	23.49	29.64	29.43	32.87	32.68	36.56

Rd	Week7	21.05	21.03	29.48	29.4	30.51	29.92	28.65	28.63	24.84	24.83	29.74	29.66	30.04	30.04	33.98
Rd	Week7	24.61	24.5	31.86	31.59	34.88	34.33	33.91	33.76	28.51	28.13	35.48	35.37	35.59	35.54	34.85
Wt	Week14	20.8	20.78	29.9	29.6	28.7	28.5	28	27.9	23.8	23.7	30	30	29.5	29.4	34.2
Wt	Week14	24.37	24.36	31.5	31.5	34.6	34	34.4	34.3	27.8	27.7	36.2	35.5	34.4	33.9	35.2
Wt	Week14	23.52	23.49	31.9	31.8	33.3	33.1	32.2	31.8	27.5	27.4	35.3	34.6	33.5	33	35.9
Rd	Week14	23.54	23.49	31.5	31.5	32.7	32.5	33.2	33	27.7	27.2	34.9	34.6	33.4	33	35.3
Rd	Week14	21.28	21.15	29.7	29.6	29.4	29.4	28.5	28.4	24.7	24.7	30.7	30.7	30.5	30.5	33.3
Rd	Week14	24.63	24.5	32.2	31.3	31.6	31.5	32.5	32.5	26.2	26.1	34.9	34.9	33.1	32.7	31.5
Wt	Weeh21	22.16	21.9	30.8	30.4	29.8	29.2	29.8	29.7	24.2	24.2	32.3	32.2	30.9	30.8	37.2
Wt	Weeh21	21.59	21.48	30.4	30.4	29.5	29.4	29.9	29.7	24.5	23.8	31.8	31.4	31	31	35.2
Wt	Weeh21	23.29	23.18	31.3	31.2	31.9	31.8	30.7	30.4	26.8	26.4	32.8	32.7	32.7	32.7	36.8
Wt	Weeh21	22.98	22.73	30.7	30.6	29.8	29.7	29.4	28.7	26.6	25.8	32.8	32.5	31	30.9	35.1
Wt	Weeh21	22.51	22.48	31.1	30.8	30	29.7	30.2	29.2	25.8	25.2	32.4	31.9	31.5	31.3	34.5
Rd	Weeh21	23.9	23.84	31.4	31.3	32.7	32.6	33.8	33.5	29.3	28.4	34.6	34	34.1	34	36.4
Rd	Weeh21	23.33	23.25	31.2	31.2	31.5	31.4	31.8	31.2	25.9	25.9	32.3	32.1	32.5	32.4	36.8
Rd	Weeh21	24.09	23.82	31.6	31.6	31.6	31.2	31.5	31.3	26.4	26.2	33.5	33.5	33.3	33.1	36.9
Rd	Weeh21	23.74	23.71	31.7	31.6	31.9	31.9	31.5	31.5	26.2	25.8	32.4	32.2	32.9	32.7	36.9
Rd	Weeh21	24.67	24.53	32.3	32.1	32.1	31.9	32.4	32.3	27.8	27.7	35.2	34.7	33.4	33.4	34.9
Wt	Week35	21.9	22.17	30.6	30.3	30.4	30.2	31.7	31.4	24.9	24.8	32.8	32.2	32	32	35.2
Wt	Week35	21.97	21.81	30.4	30.2	31.1	31	28.8	28.7	23.9	23.4	30.6	30.6	30.7	30.6	35.2
Wt	Week35	21.92	21.91	30.5	30.5	30.8	30.3	29.6	29.4	26.1	26.1	31.4	31.1	31.3	31	35.2
Rd	Week35	22.53	22.42	30.8	30.8	33.5	33	32.6	32.4	25.3	25.2	33.8	33.5	32.8	32.5	37.4
Rd	Week35	21.49	21.45	30.1	30.1	30.4	30.2	29.4	29.1	24	24	31.7	31.6	31.2	31.1	34.7
Rd	Week35	23.56	23.37	31.7	31.5	32	31.8	32.7	32.6	26.8	26.5	34.6	34.3	33.6	33.6	35.9

Appendix 5: Syntax for Correlation Analysis

```
SORT CASES BY Age(A).  
SPLIT FILE SEPARATE BY Age.  
CORRELATIONS  
  /VARIABLES=GAPDHhi GAPDHlow  
  /PRINT=TWOTAIL NOSIG  
  /MISSING=PAIRWISE.
```

Appendix 6: $\Delta\Delta\text{Ct}$ values for all genes for wt mice

Geno type	Age	$\Delta\Delta\text{CtFurin}$	$\Delta\Delta\text{CtPACE4}$	$\Delta\Delta\text{CtPC1}$	$\Delta\Delta\text{CtPC2}$	$\Delta\Delta\text{CtPC5}$	$\Delta\Delta\text{CtPC7}$
Wt	Week1	1.97	0.71	-2.26	-0.92	0.6	0.24
Wt	Week1	1.19	1.08	-2.41	0.16	0.39	0.61
Wt	Week1	1.1	1.58	-2.06	1.47	1.27	1.06
Wt	Week2	0.16	-0.27	-0.9	-0.33	-0.44	-0.36
Wt	Week2	-0.16	-0.34	-1.02	-0.21	-0.38	0.14
Wt	Week2	-0.78	0.07	-0.49	0.25	0.63	-0.36
Wt	Week3	-0.13	0.15	-0.23	-0.68	-0.28	-0.5
Wt	Week3	-0.5	0.44	-0.11	0.27	0.34	-0.07
Wt	Week3	-1.36	0.9	0.87	1.34	1.44	0.43
Wt	Week4	0.77	0.06	-0.95	-0.72	-1.16	-0.88
Wt	Week4	-0.3	-0.14	-1.8	-0.87	-1.17	-0.96
Wt	Week4	-1.55	0.33	-1.19	0.48	-0.41	-0.46
Wt	Week5	-0.09	-0.13	-1.74	-1.74	-1.47	-1.44
Wt	Week5	-0.53	-0.05	-1.54	-0.6	-1.49	-1.18
Wt	Week5	-0.8	-0.39	-3.08	-0.19	-2.34	-2.42
Wt	Week6	0.85	0.41	-1.83	-0.27	-0.39	-0.89
Wt	Week6	0.79	0.31	-1.42	0.76	-0.41	-0.63
Wt	Week6	-0.11	0.78	-0.48	1.74	-1.02	-0.37
Wt	Week7	-0.29	1.29	1.06	-0.54	-0.36	-0.08
Wt	Week7	-0.39	0.16	0.57	-0.72	-0.01	0.02
Wt	Week7	-1.46	0.58	2.4	0.15	0.43	0.55
Wt	Week14	1.22	0.41	-0.32	-1.21	-0.48	0.09
Wt	Week14	0.05	-1.09	-0.97	-0.57	-2.09	-0.46
Wt	Week14	-0.37	-0.8	-0.48	0.23	-0.98	0.2
Wt	Week21	-0.04	0.82	-0.37	-1.28	-0.78	-0.13
Wt	Week21	-0.15	1.17	0.21	-0.5	-0.27	-0.16
Wt	Week21	-0.3	1.25	1.8	0.82	0.7	0.49

Appendix 7: $\Delta\Delta$ Ct values for all genes for Rd mice

Geno type	Age	$\Delta\Delta$ CtFurin	$\Delta\Delta$ CtPACE4	$\Delta\Delta$ CtPC1	$\Delta\Delta$ CtPC2	$\Delta\Delta$ CtPC5	$\Delta\Delta$ CtPC7
Rd	Week1	-1.94	-3.06	-1.97	1.46	-0.51	-2.8
Rd	Week1	-1.51	-3.36	-1.93	-1.2	-1.29	-2.84
Rd	Week1	-2.17	-4.51	-1.63	-1.49	-3.03	-3.54
Rd	Week2	0.6	0.18	-1.32	-0.87	-0.02	-0.76
Rd	Week2	0.67	0.35	-0.58	-0.85	0.05	-0.84
Rd	Week2	0.96	-0.03	0.45	0	0.09	0.24
Rd	Week3	1.42	0.38	-0.11	0.38	0.51	0
Rd	Week3	0.62	0.39	0.11	-0.06	0.38	0.01
Rd	Week3	0.96	0.39	0.66	0.21	-0.32	-0.93
Rd	Week4	0.06	0.05	0.48	0.21	0.64	0.57
Rd	Week4	0.56	0.43	1.67	0.81	0.67	0.41
Rd	Week4	1.5	0.14	2.42	-0.13	0.45	-0.33
Rd	Week5	1.01	1.39	1.04	0.98	1.56	1.05
Rd	Week5	0.62	1.16	1.08	0.64	1.52	1.16
Rd	Week5	0.95	-0.46	2.24	1.54	2.61	1.34
Rd	Week6	0.37	-0.03	1.17	-0.46	0.1	-0.13
Rd	Week6	0.01	-0.12	0.59	-0.45	0.5	0.09
Rd	Week6	0.81	-0.18	1.01	-0.35	1.7	0.14
Rd	Week7	0.39	-2.2	-0.86	-0.59	0.87	-0.11
Rd	Week7	0.47	-1.39	0.22	0.46	0.75	-0.07
Rd	Week7	1.29	-1.42	0.16	0.82	0.94	-0.16
Rd	Week14	-0.02	0.81	-0.05	1.39	-0.29	0.38
Rd	Week14	0.39	1.53	0.59	-0.06	1.13	0.45
Rd	Week14	0.55	0.89	0.41	0.06	0.24	0.05
Rd	Week21	0.94	-0.75	-0.23	0.78	-0.06	-0.15
Rd	Week21	1	-0.73	-0.41	1	-0.72	0.28
Rd	Week21	1.21	-0.85	-0.09	0.78	-0.62	0.23
Rd	Week35	0.25	-0.2	-0.96	-0.78	-1.46	-0.96
Rd	Week35	0.09	-0.18	-1.67	0.07	-1.64	-0.87
Rd	Week35	-0.04	-1.57	-0.51	0.99	-0.69	-0.21

Appendix 8: Syntax for Bonferroni post-hoc pairwise comparisons

* prestg80 is your continuous duration outcome for a given behavior .

* sex is GROUP .

* race is AGE .

UNIANOVA

DeltaDeltaCTAve BY Genotype Age

/METHOD = SSTYPE(3)

/INTERCEPT = INCLUDE

/SAVE = PRED RESID COOK

/EMMEANS = TABLES(Age) COMPARE ADJ(BONFERRONI)

/PRINT = DESCRIPTIVE ETASQ OPOWER PARAMETER HOMOGENEITY

/CRITERIA = ALPHA(.05)

/DESIGN = Age Genotype Genotype*Age.

* assess correlation of student and computer measures of a given behavior .